FINNISH METEOROLOGICAL INSTITUTE

HELSINGIN YLIOPISTO
HELSINGFORS UNIVERSITET
UNIVERSITY OF HELSINKI

Millaista on hengittää Kiinassa?
Katsaus Itä-Kiinan pienhiukkastutkimukseen

Aki Virkkula
Ilmatieteen laitos & Helsingin yliopisto

Sisältö

Millaista on hengittää Kiinassa?
- ❑ Pitoisuuksia
- ❑ Terveysvaikutuksia

Pitoisuuksien trendejä
- ❑ Satelliittidatasta

Subjektiivinen katsaus Itä-Kiinan pienhiukkastutkimukseen
- ❑ Suuren mittakaavan kenttäkokeita
- ❑ Joitain tuloksia artikkeleista, joissa olen yhtenä kirjoittajana
- ❑ SORPES

Introduction: Air Pollution in China

Kristin Aunan*, Mette Halskov Hansen† and Shuxiao Wang‡

The China Quarterly, 234, 279–298, 2018

Figure 2: **Annual Average $PM_{2.5}$ Concentrations in China in 2015**

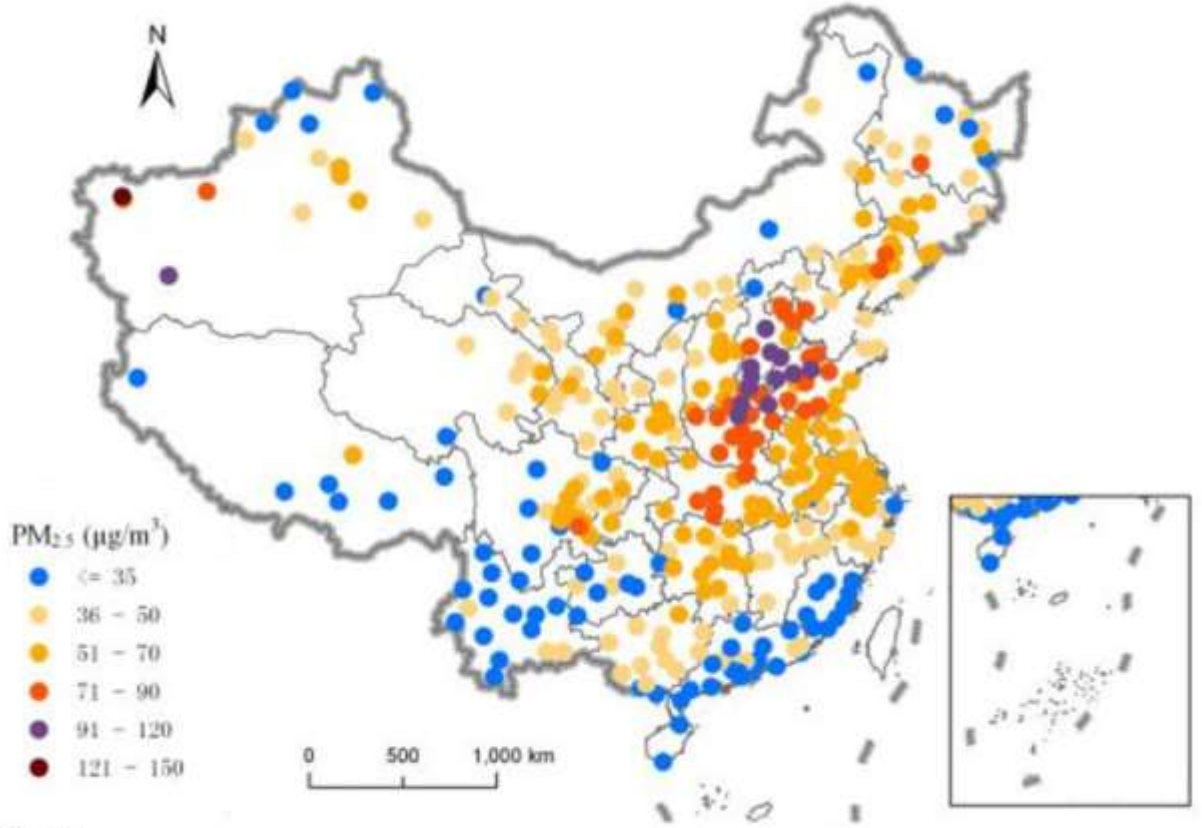

Source:
Annual average values based on hourly data downloaded from China National Environment Monitoring Center http://106.37.208.233:20035/. Accessed 27 April 2016.

$PM_{2.5}$ –vuosikeskiarvojen maantieteellinen jakauma

Satelliittidatasta arvioitu $PM_{2.5}$ -pitoisuus

van Donkelaar et al.: Global estimates of average ground-level fine particulate matter concentrations from satellite-based aerosol optical depth, *Environ. Health Perspect.*, 847–855, 2010.

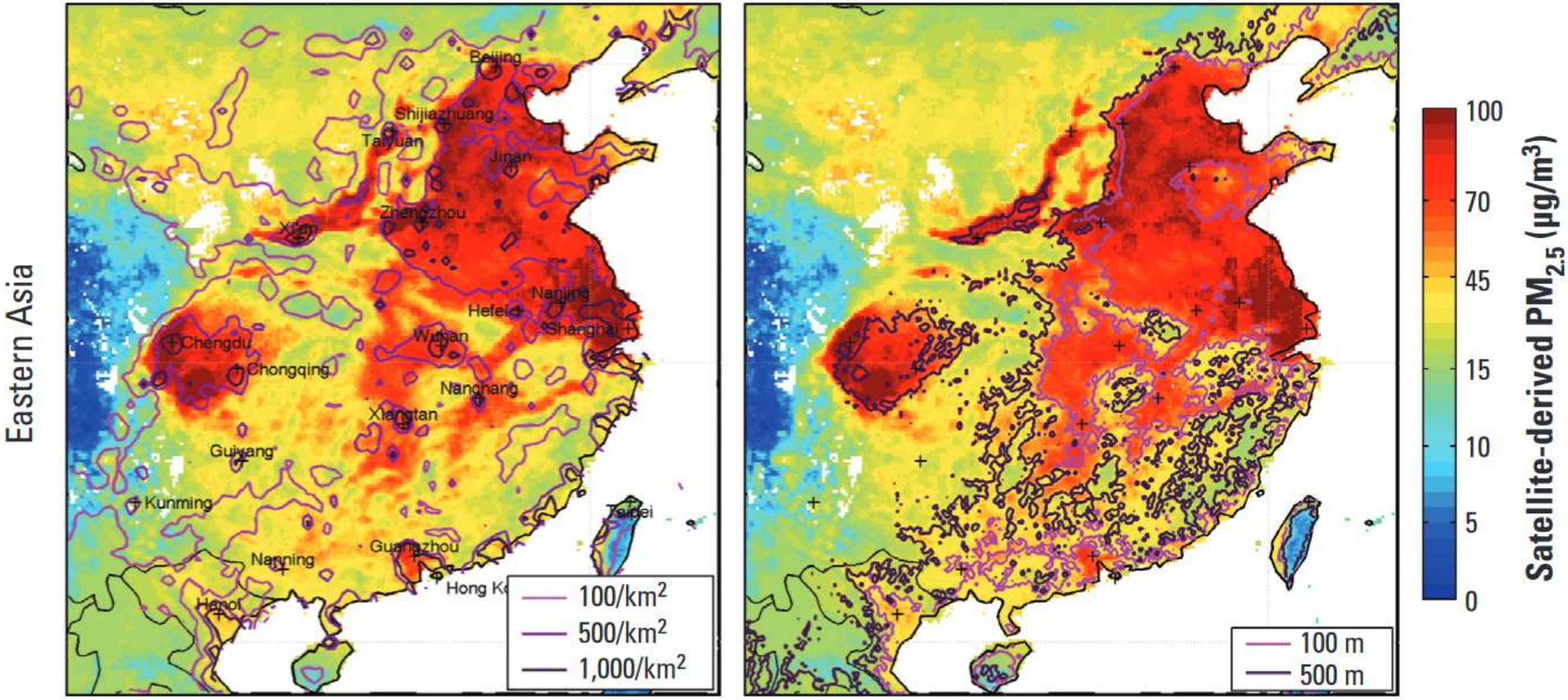

Figure 5. Regional satellite-derived $PM_{2.5}$ concentrations. Columns show mean satellite-derived $PM_{2.5}$ for 2001–2006 at locations that contain at least 50 measurements. Contours denote population density (left) and surface elevation (right). Crosses indicate city centers. Note the different color scales for each region. Altitude data are from the U.S. Geological Survey (1996).

Rohde RA, Muller RA (2015) Air Pollution in China: Mapping of Concentrations and Sources.
PLoS ONE 10(8): e0135749. doi:10.1371/journal, pone.0135749

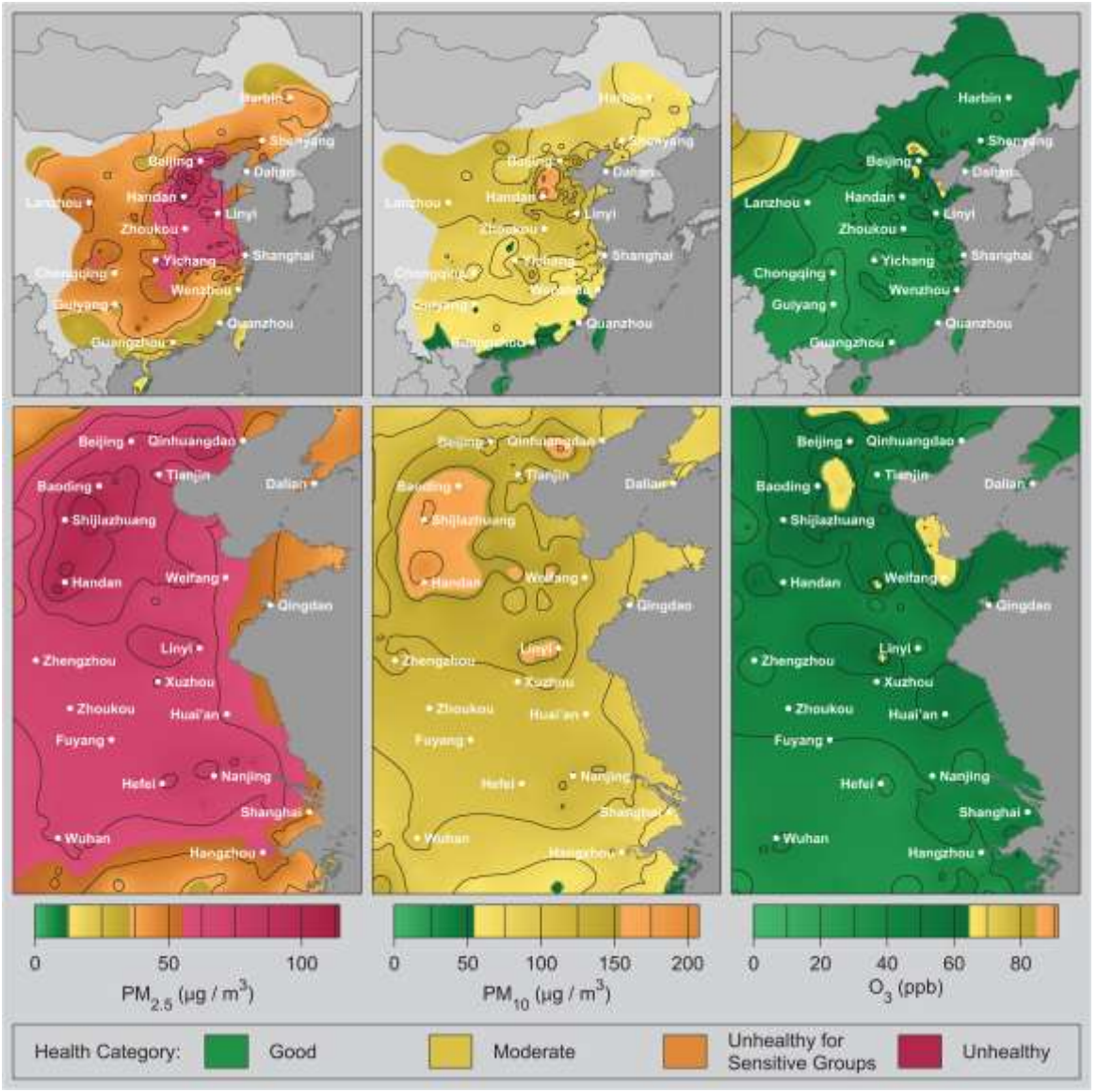

Fig 3. Average air pollution maps. Maps of average pollutant concentration for $PM_{2.5}$, PM_{10}, and O_3 for eastern China (top row) and the Beijing to Shanghai corridor (bottom row).

Seuraavilla sivuilla esitetään pitoisuuksia Nanjingin yliopiston Xianlinin kampuksella sijaitsevalla ”*Station for Observing Regional Processes of the Earth System*” (SORPES) -mittausasemalla

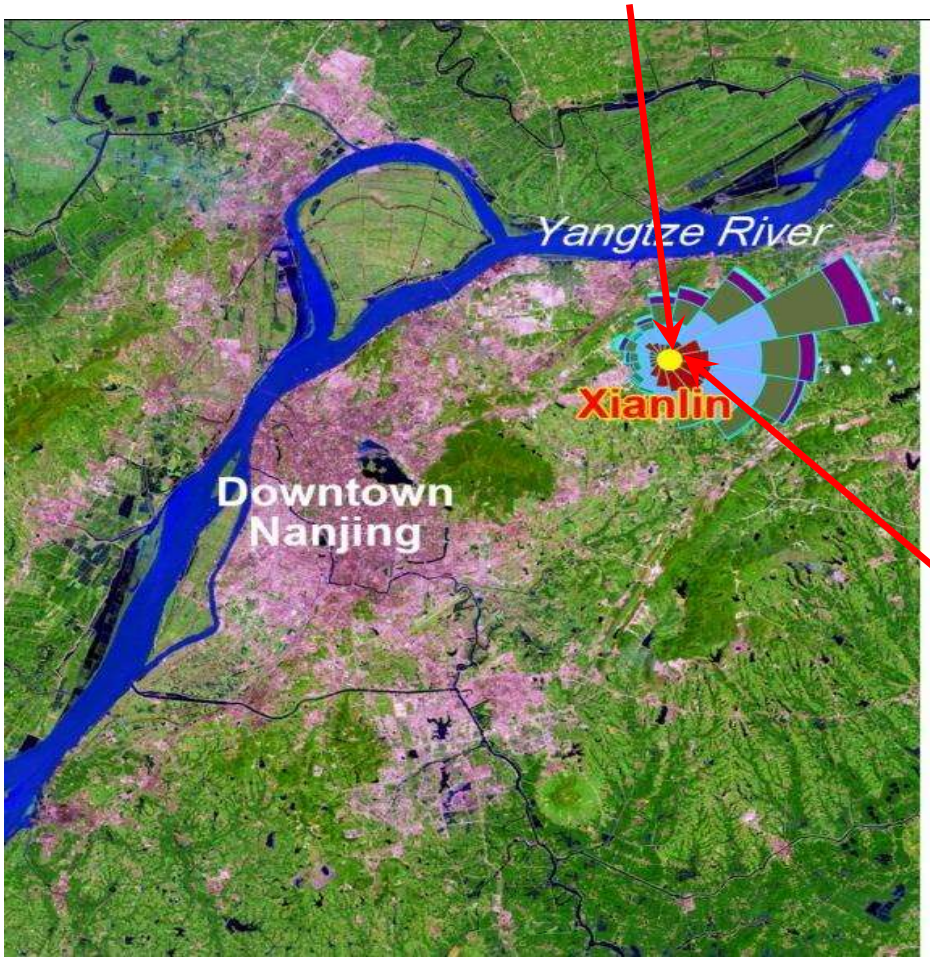

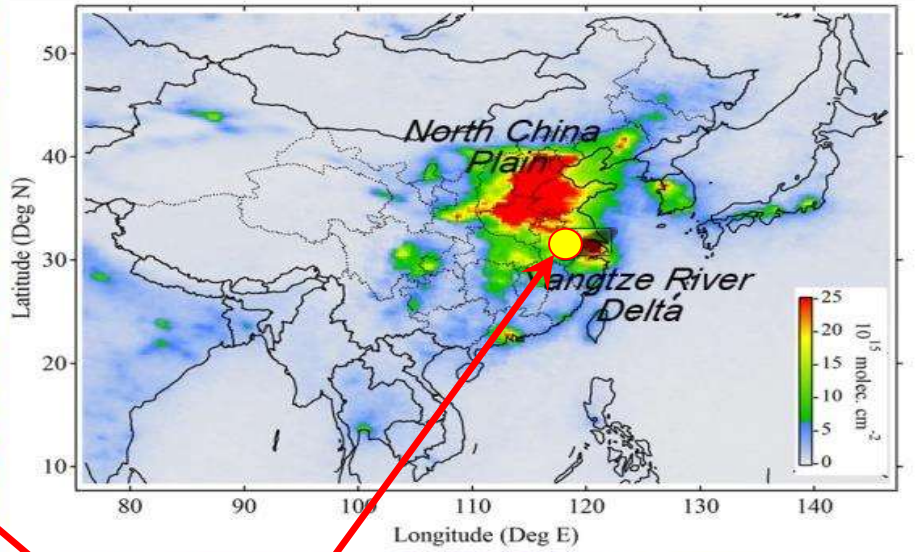

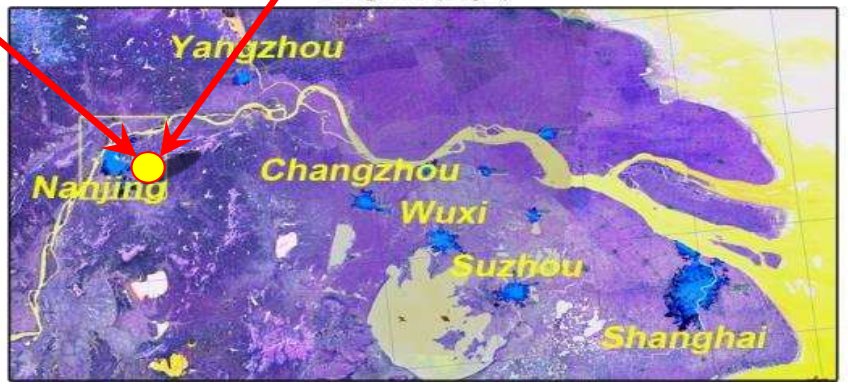

Pitoisuustasoista

Esimerkkinä vertailu:

$PM_{2.5}$-pitoisuuksia

- SORPES, Nanjing 2013/07 – 2015/05 (Shen et al., ACP 2018)
- Helsinki, Mannerheimintie, 2015/09 – 2017/12
- Kittilä, Matorova, 2015/09 – 2017/12

(Hki & Kittilä: http://ilmatieteenlaitos.fi/havaintojen-lataus)

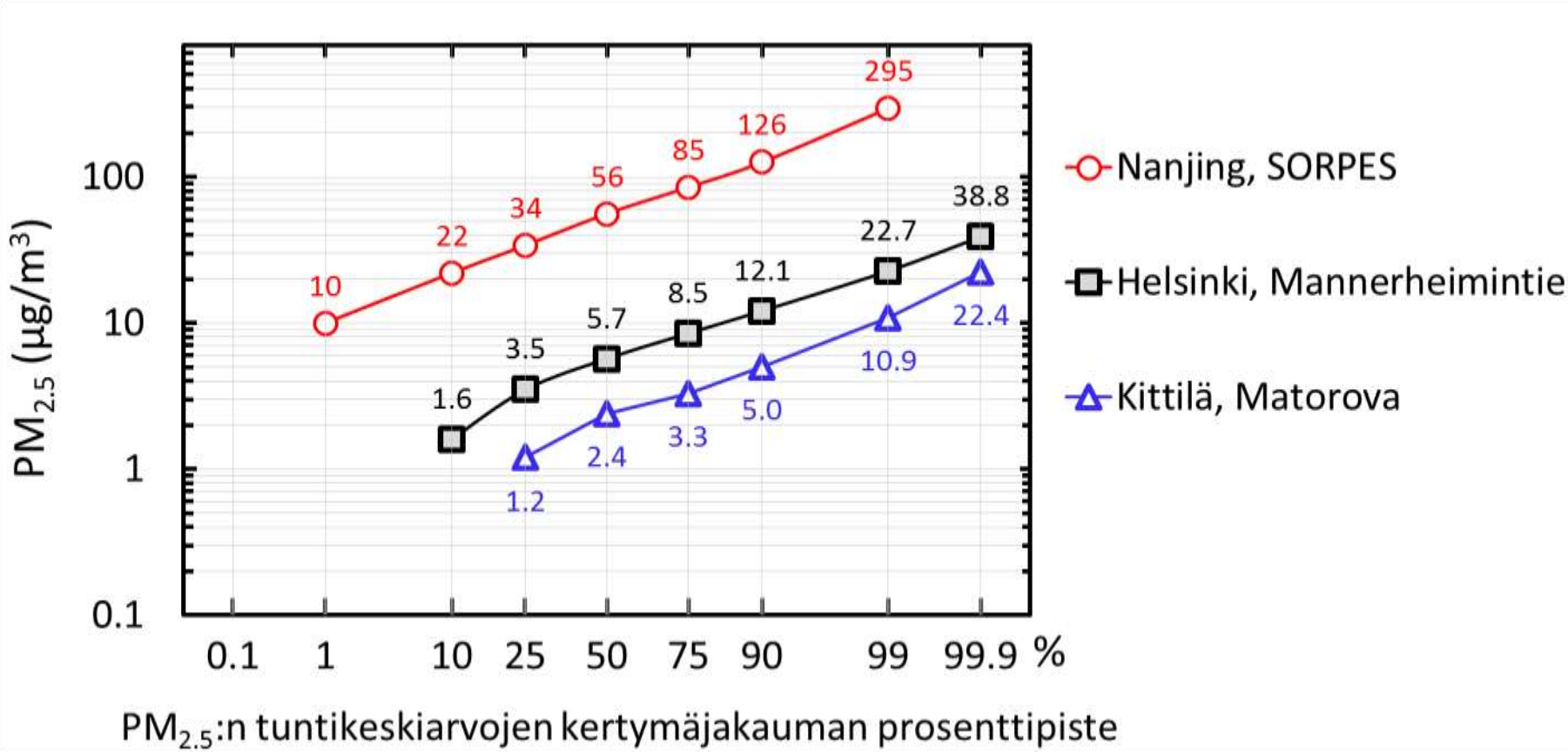

http://aqicn.org –sivustolla ilmanlaatuindeksi lasketaan US EPAn kaavalla

$$I_p = \frac{I_{Hi} - I_{Lo}}{BP_{HI} - BP_{Lo}}(C_p - BP_{Lo}) + I_{Lo}$$

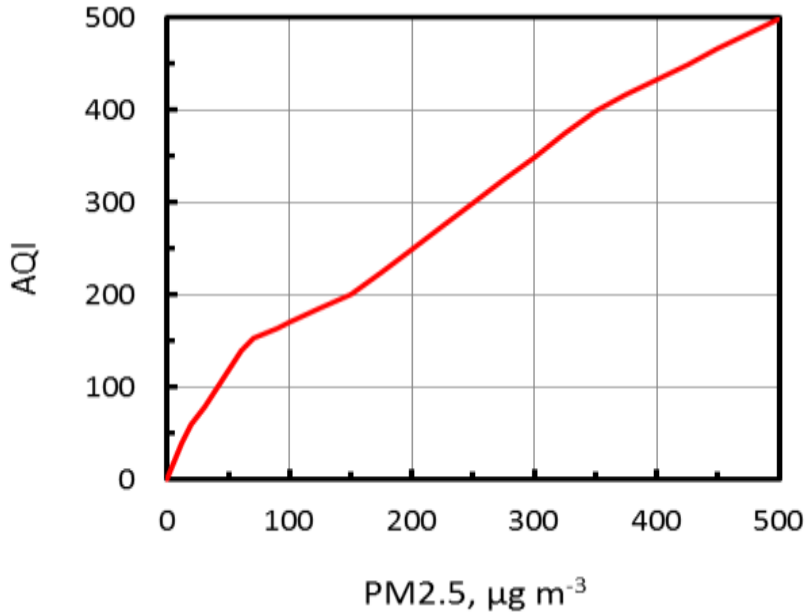

Air Quality Index

AQI	Air Pollution Level	Health Implications
0 - 50	Good	Air quality is considered satisfactory, and air pollution poses little or no risk
51 -100	Moderate	Air quality is acceptable; however, for some pollutants there may be a moderate health concern for a very small number of people who are unusually sensitive to air pollution.
101-150	Unhealthy for Sensitive Groups	Members of sensitive groups may experience health effects. The general public is not likely to be affected.
151-200	Unhealthy	Everyone may begin to experience health effects; members of sensitive groups may experience more serious health effects
201-300	Very Unhealthy	Health warnings of emergency conditions. The entire population is more likely to be affected.
300+	Hazardous	Health alert: everyone may experience more serious health effects

$PM_{2.5}$-pitoisuuksista laskettu AQI

- SORPES, Nanjing 2013/07 – 2015/05 (Shen et al., ACP 2018)
- Helsinki, Mannerheimintie, 2015/09 – 2017/12
- Kittilä, Matorova, 2015/09 – 2017/12
  (Hki & Kittilä: http://ilmatieteenlaitos.fi/havaintojen-lataus)

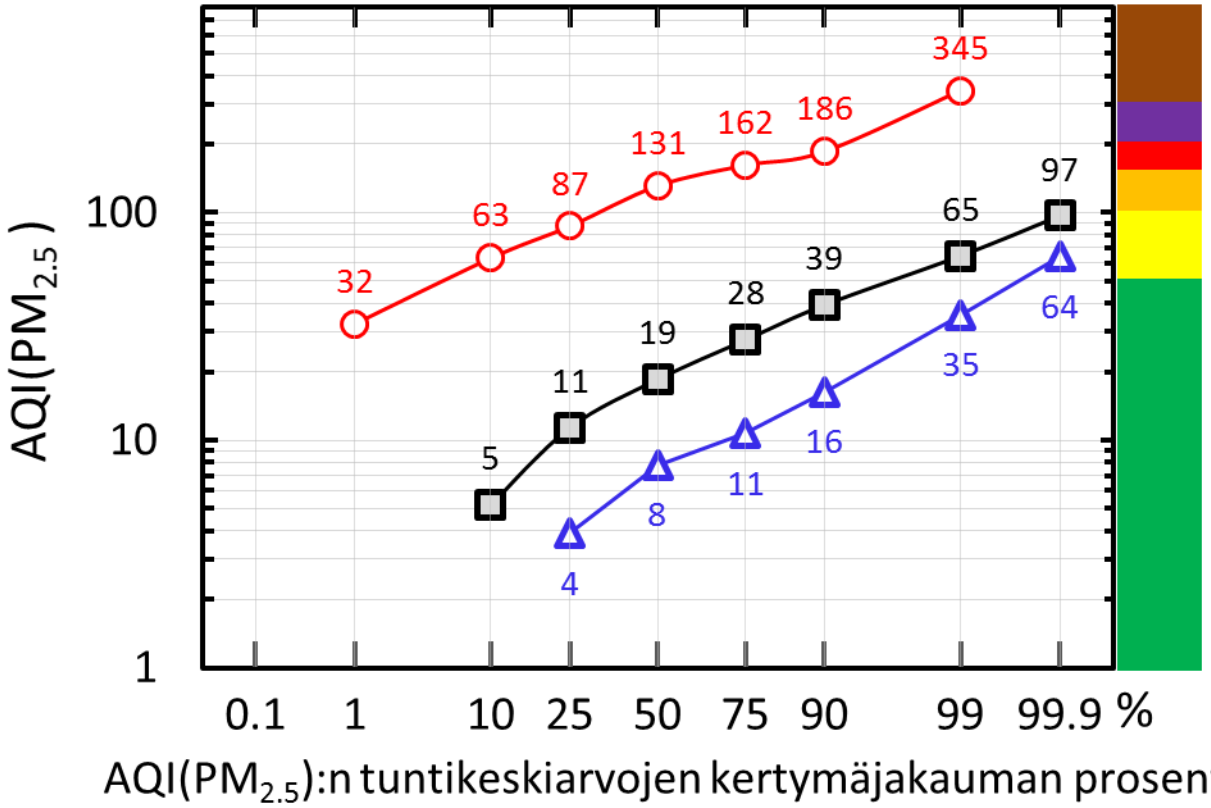

AQI	Air Pollution Level
0 - 50	Good
51 -100	Moderate
101-150	Unhealthy for Sensitive Groups
151-200	Unhealthy
201-300	Very Unhealthy
300+	Hazardous

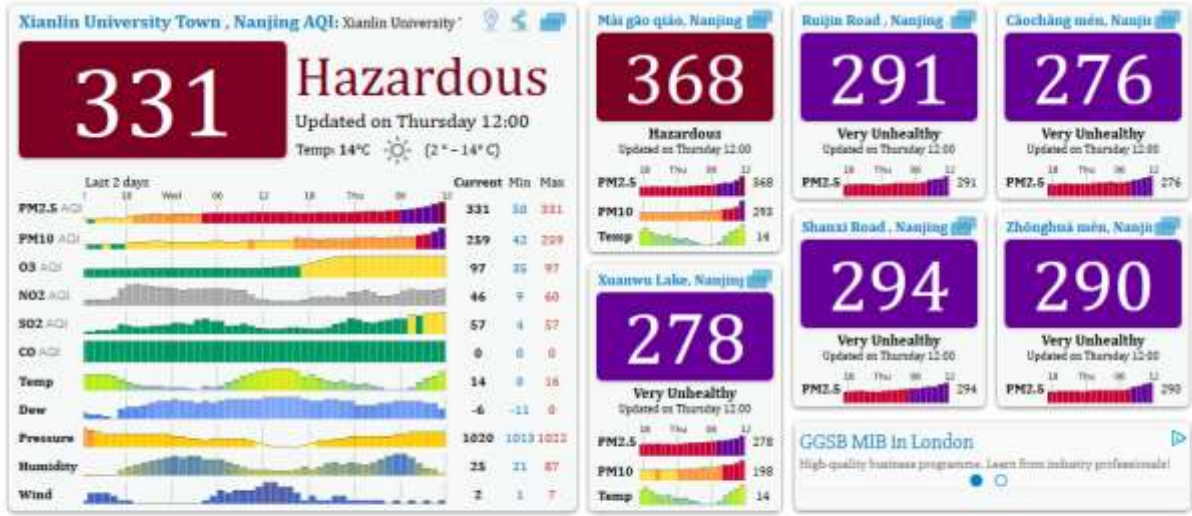
Xianlin University Town , Nanjing AQI: Xianlin University
331
Hazardous
Updated on Thursday 12:00
Temp: 14°C (2° - 14° C)
Last 2 days
Current Min Max
PM2.5 AQI 331 10 331
PM10 AQI 259 42 259
O3 AQI 97 35 97
NO2 AQI 46 9 60
SO2 AQI 57 4 57
CO AQI 0 0 0
Temp 14 8 16
Dew -6 -11 0
Pressure 1020 1013 1022
Humidity 25 21 87
Wind 2 1 7
Mài gāo qiáo, Nanjing
368
Hazardous
Updated on Thursday 12:00
PM2.5 368
PM10 293
Temp 14
Ruijin Road , Nanjing
291
Very Unhealthy
Updated on Thursday 12:00
PM2.5 291
Cáochāng mén, Nanjin
276
Very Unhealthy
Updated on Thursday 12:00
PM2.5 276
Xuanwu Lake, Nanjing
278
Very Unhealthy
Updated on Thursday 12:00
PM2.5 278
PM10 198
Temp 14
Shanxi Road , Nanjing
294
Very Unhealthy
Updated on Thursday 12:00
PM2.5 294
Zhōnghuá mén, Nanjin
290
Very Unhealthy
Updated on Thursday 12:00
PM2.5 290
GGSB MIB in London
High-quality business programme. Learn from industry professionals!


Nanjing, China Nearest Air Quality monitoring stations
World
Asia
Europe
North America
South America
Australia
Middle East
China
368
331
278
294
290
276
291
296
290
南京市

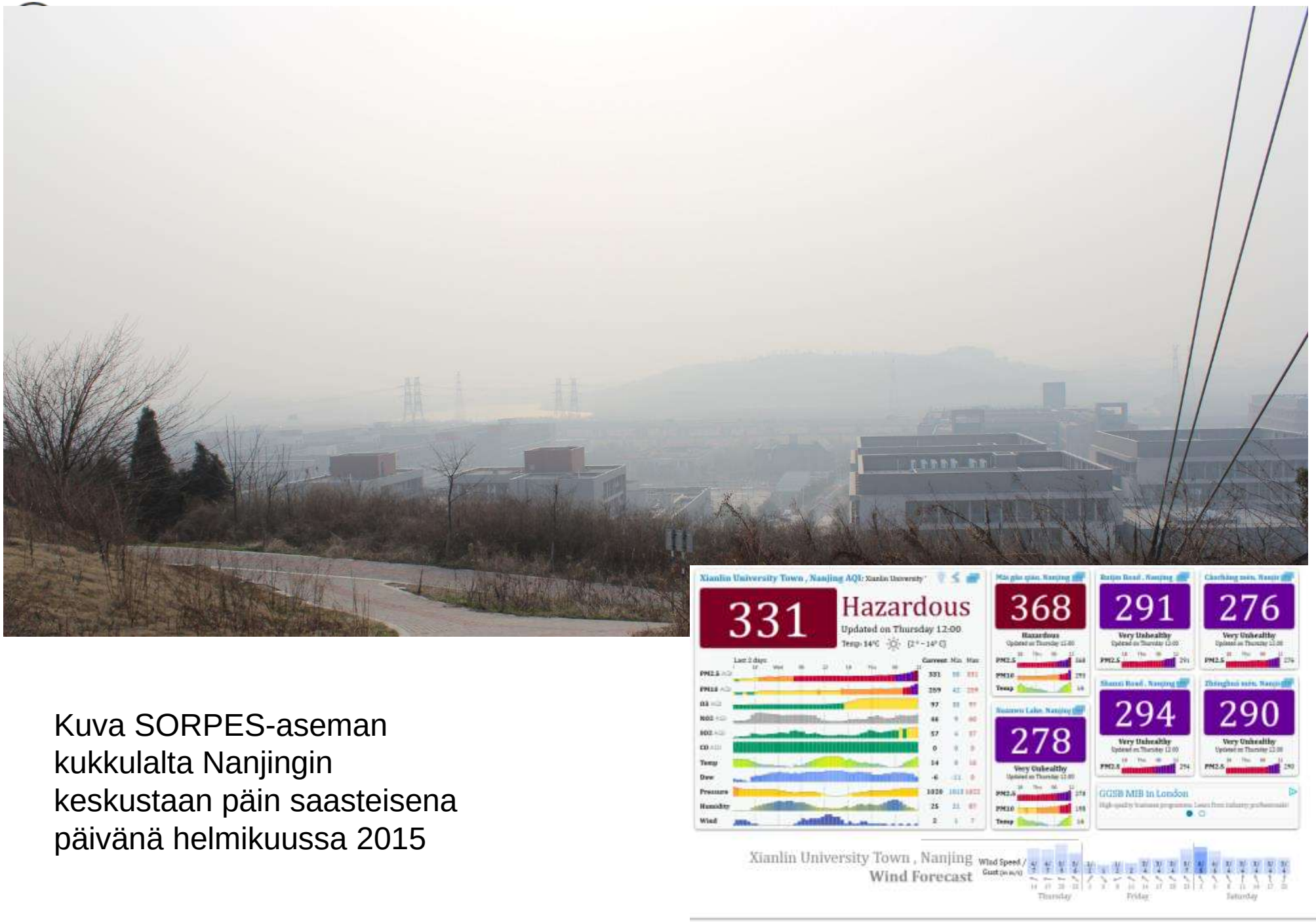

Kuva SORPES-aseman kukkulalta Nanjingin keskustaan päin saasteisena päivänä helmikuussa 2015

Kuva SORPES-aseman kukkulalta Nanjingin keskustaan päin puhtaana päivänä helmikuussa 2015

Vertailu Dockery et al. (1993) ”Six-city study” –julkaisun pitoisuuksiin

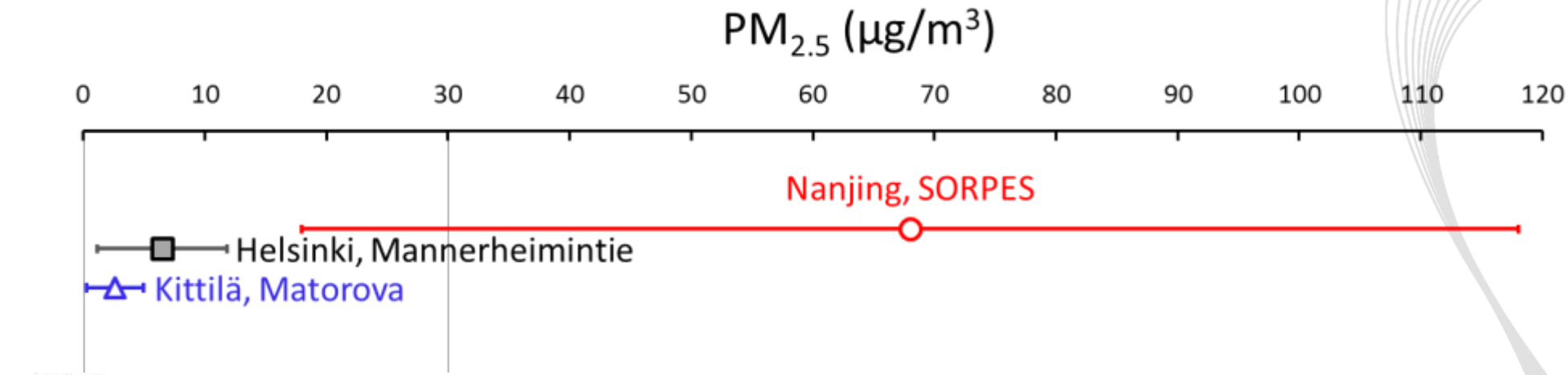

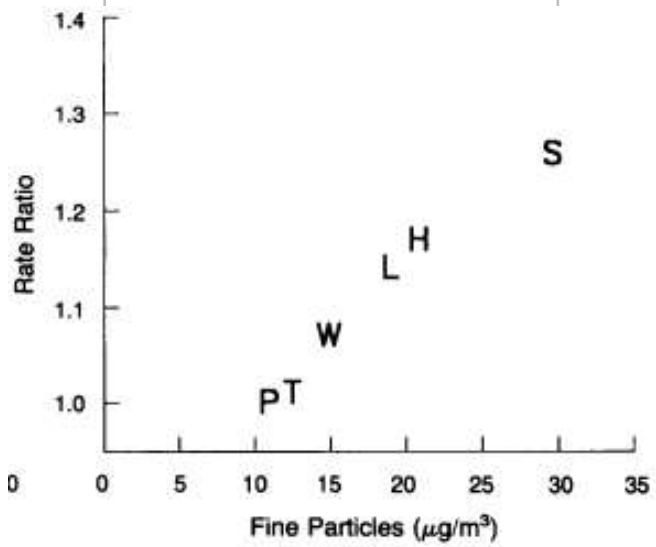

The New England
Journal of Medicine

Volume 329 DECEMBER 9, 1993 Number 24

AN ASSOCIATION BETWEEN AIR POLLUTION AND MORTALITY IN SIX U.S. CITIES

Douglas W. Dockery, Sc.D., C. Arden Pope III, Ph.D., Xiping Xu, M.D., Ph.D.,
John D. Spengler, Ph.D., James H. Ware, Ph.D., Martha E. Fay, M.P.H.,
Benjamin G. Ferris, Jr., M.D., and Frank E. Speizer, M.D.

Figure 3. Estimated Adjusted Mortality-Rate Ratios and Pollution Levels in the Six Cities.
Mean values are shown for the measures of air pollution. P denotes Portage, Wisconsin; T Topeka, Kansas; W Watertown, Massachusetts; L St. Louis; H Harriman, Tennessee; and S Steubenville, Ohio.

Guan W.-J., Zheng, X.-Y., Chung, K.F., Zhong, N.-S.:

Impact of air pollution on the burden of chronic respiratory diseases in China: time for urgent action,

Lancet 2016; 388: 1939–51

Kuolleisuuden ilmansaasteisiin arvioidaan yhä nousevan, vaikka pitoisuuksissa jo trendiä alaspäin.

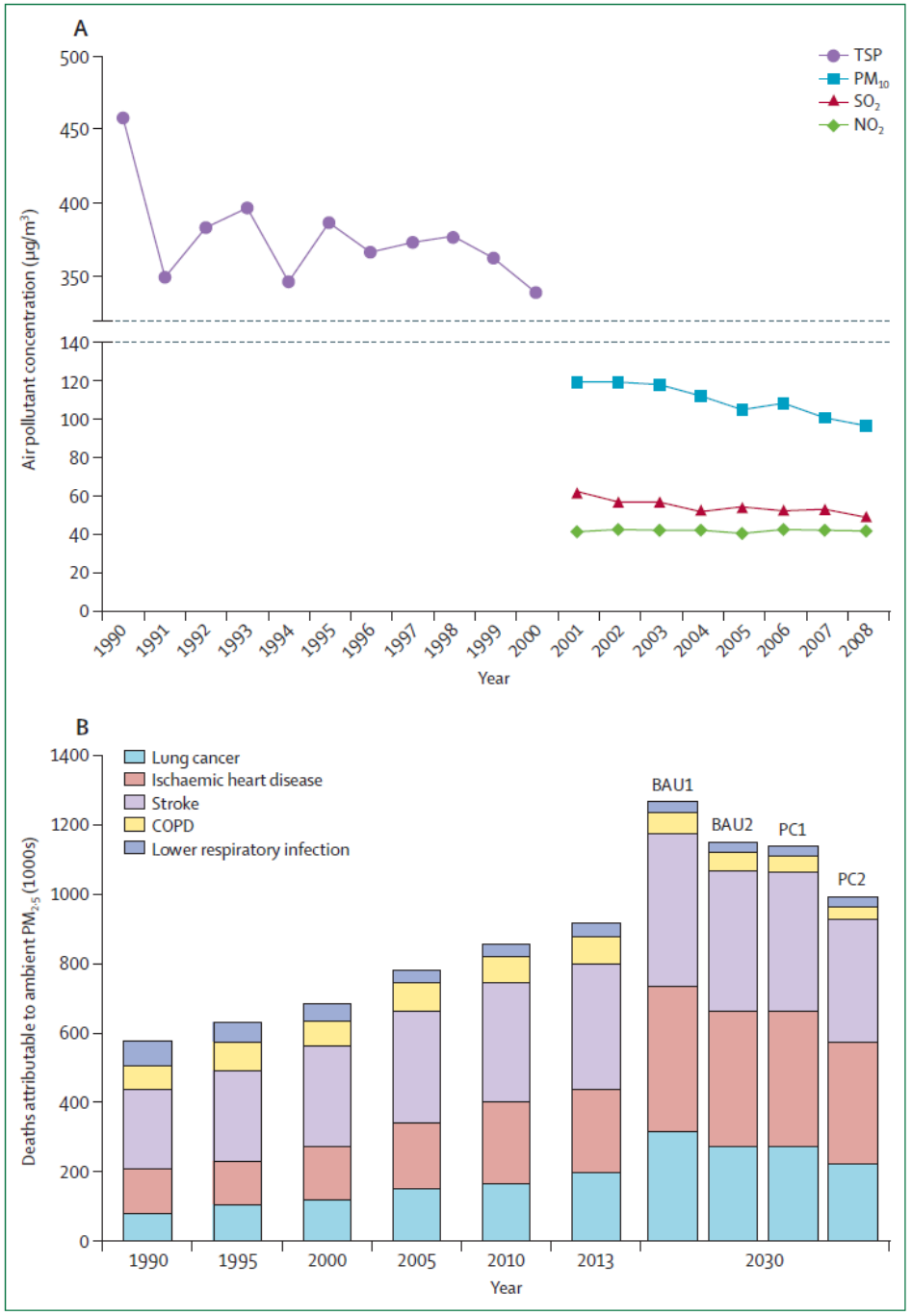

Figure 1: Air pollution concentrations and effect on mortality in China

Song et al.: Health burden attributable to ambient $PM_{2.5}$ in China, *Environ. Poll.* 223, 575 – 586, 2017.

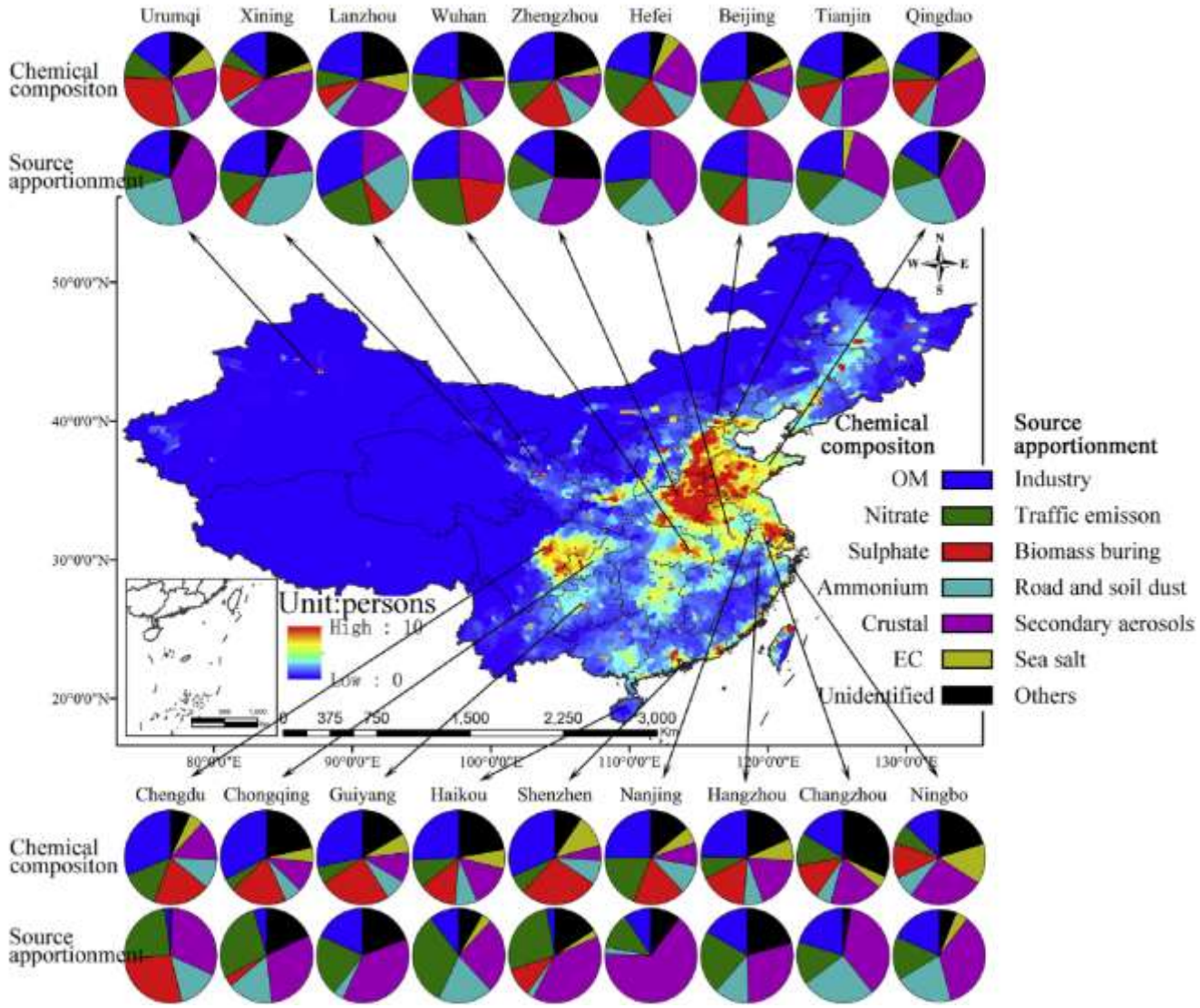

Fig. 7. Spatial distribution (0.1° x 0.1) of total mortalities attributable to $PM_{2.5}$ in 2015, chemical composition and source apportionment of $PM_{2.5}$

$PM_{2.5}$ –pitoisuuksista johtuvan kuolleisuuden maantieteellinen jakauma, hiukkasten kemiallinen koostumus ja lähteet vuonna 2015.

FINNISH METEOROLOG

Spatial and temporal trends in the mortality burden of air pollution in China: 2004–2012

Miaomiao Liu [a], Yining Huang [a], Zongwei Ma [a], Zhou Jin [a], Xingyu Liu [a], Haikun Wang [a], Yang Liu [b], Jinnan Wang [a,c], Matti Jantunen [d], Jun BiDr [a,*], Patrick L. KinneyDr [e,**]

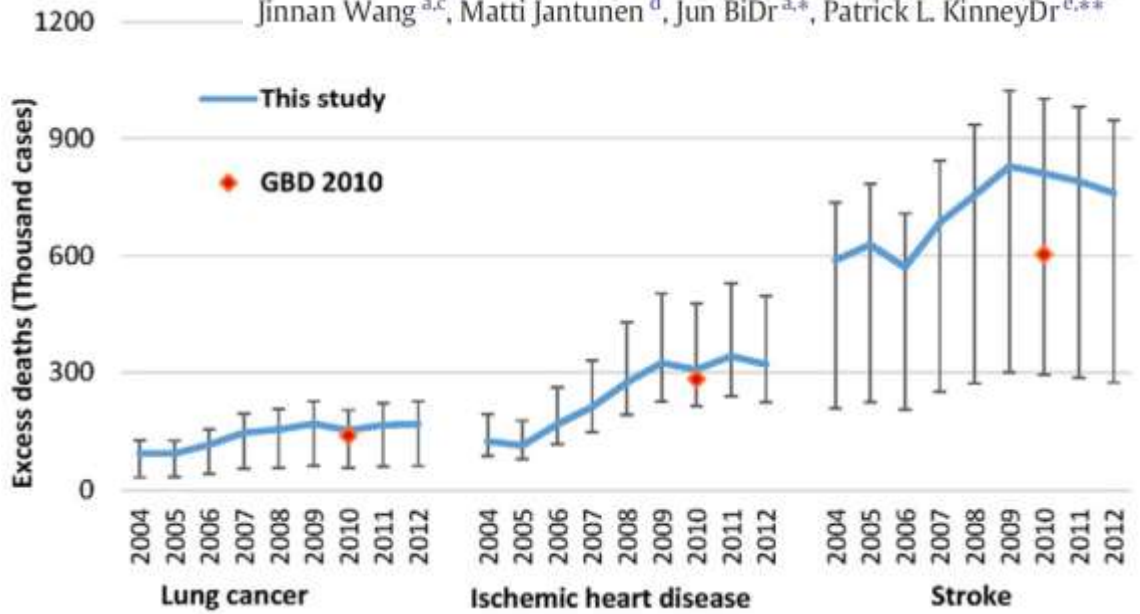

Ilmansaasteista johtuvan kuolleisuuden maantieteellinen jakauma ja trendi 2004 - 2012

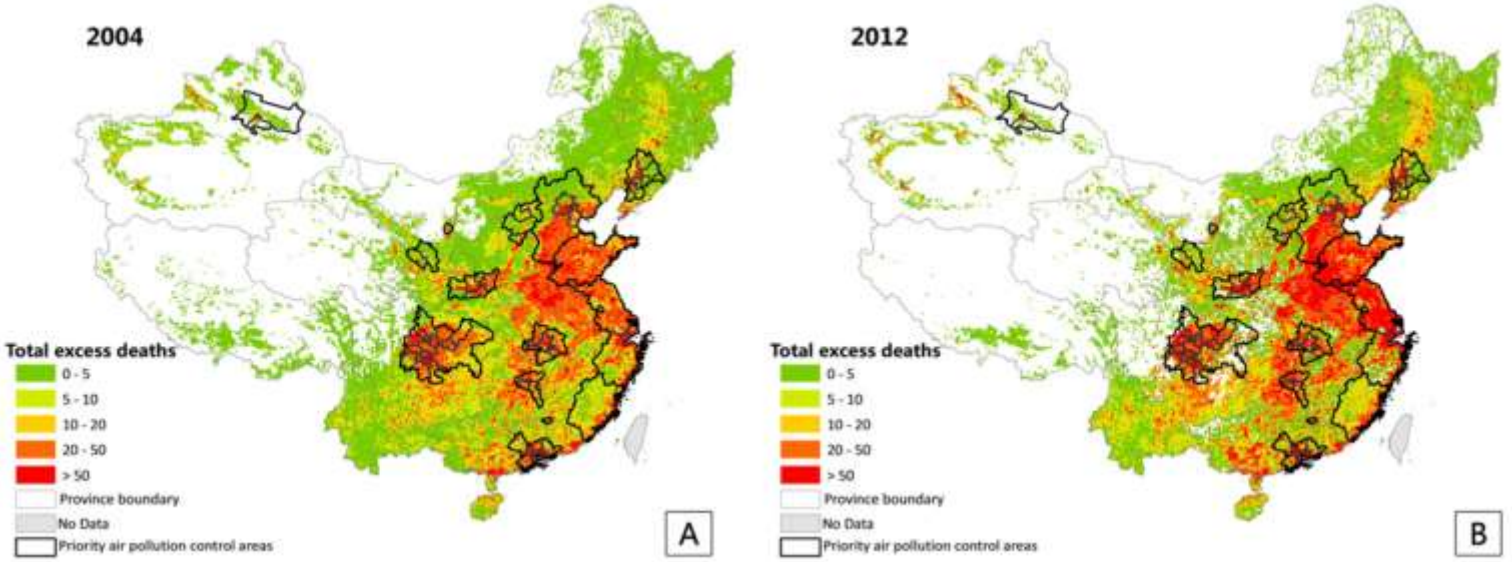

M. Liu et al. / Environment International 98 (2017) 75–81

Guo *et al*.: The association between lung cancer incidence and ambient air pollution in China: A spatiotemporal analysis, *Environ. Res.* 144, 60–65, 2016

Kiinassa esiintyy eniten keuhkosyöpää

1. Introduction

Lung cancer is now the most common cancer in the world, with the majority of the cases in developing countries (Ferlay et al., 2010; Jemal et al., 2011). China has the highest lung cancer burden in the world (Zhao et al., 2010). According to the latest Chinese cancer registration annual report, the world age-standardized incidence rate of lung cancer was 47.5 per 100,000 for men and 22.2 per 100,000 for women in 2009 (Chen et al., 2013), and these incidences are expected to rise (Chen et al., 2011).

Guo *et al*.: The association between lung cancer incidence and ambient air pollution in China: A spatiotemporal analysis, *Environ. Res.* 144, 60–65, 2016

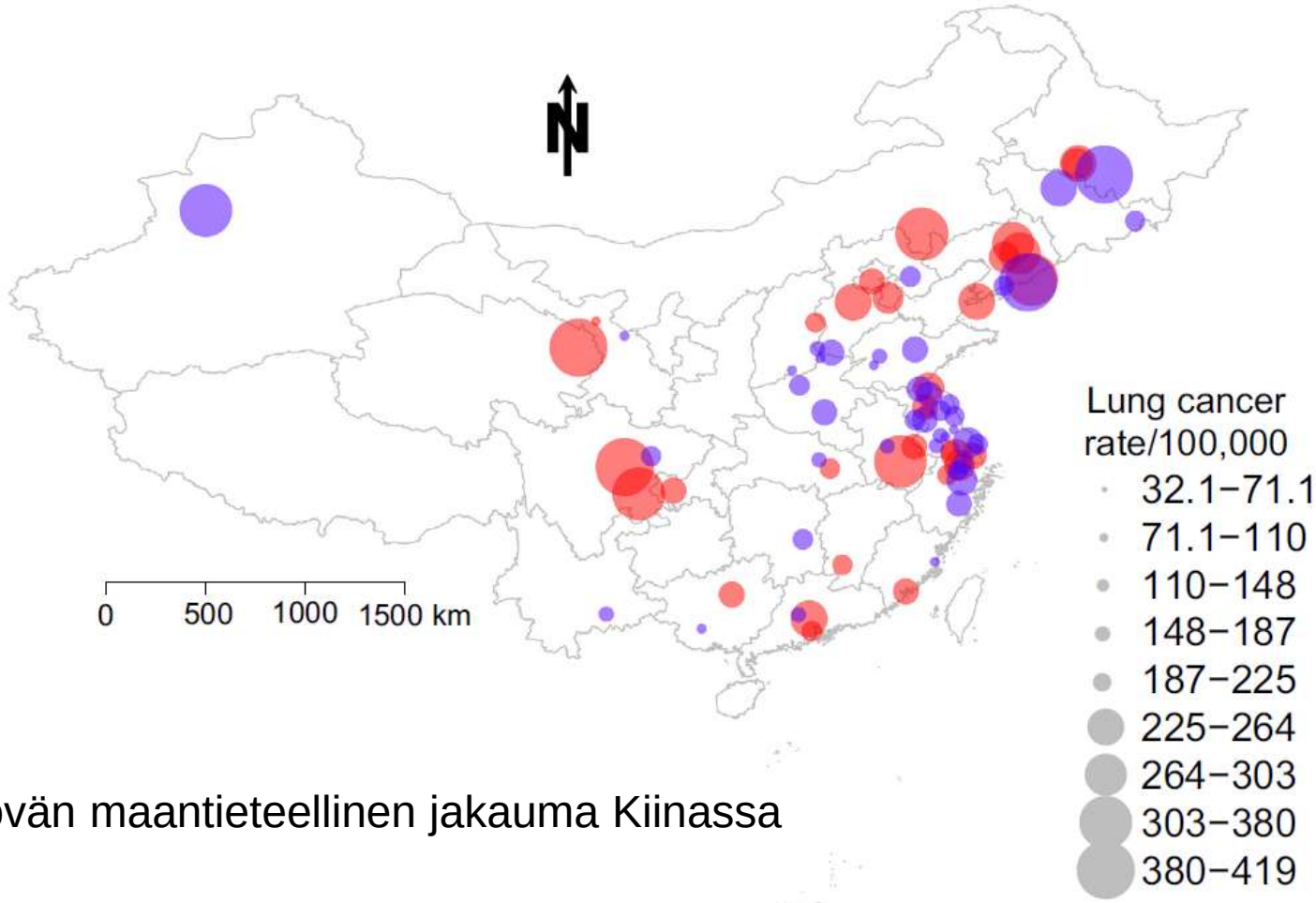

Keuhkosyövän maantieteellinen jakauma Kiinassa

Fig. 1. The location of the 75 study communities and standardized lung cancer incidence rate for people aged >30 years in urban (red colour) and rural (purple colour) China, during 1990–2009. The rate was standardized by world Segi's population 1985. (For interpretation of the references to colour in this figure legend, the reader is referred to the web version of this article.)

Guo *et al*.: The association between lung cancer incidence and ambient air pollution in China: A spatiotemporal analysis, *Environ. Res.* 144, 60–65, 2016

Keuhkosyöpä ja ilmansaasteet: sekä hiukkasilla että otsonilla positiivinen korrelaatio

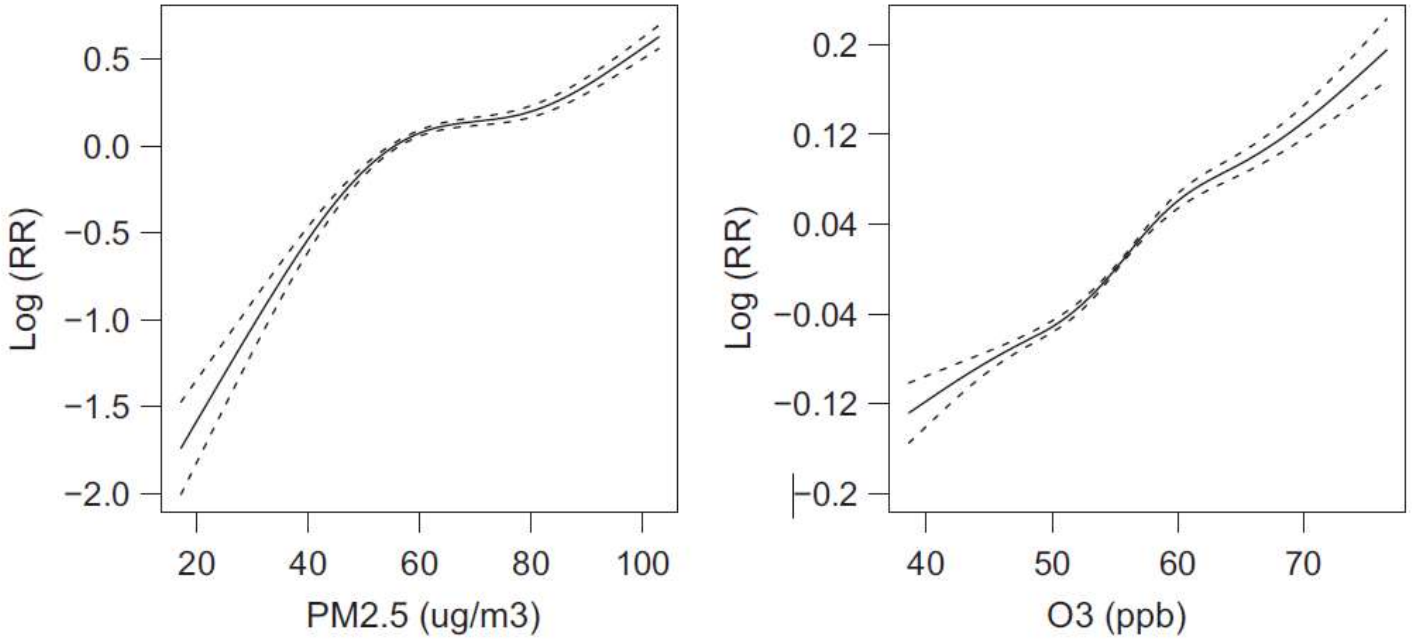

Fig. 3. : The associations between $PM_{2.5}$, O_3 and lung cancer incidence in China during 1990–2009, using spatial age-period-cohort design. A natural cubic spline with 4 degrees of freedom was used for $PM_{2.5}$ and O_3, respectively.

Ilman epäpuhtauksilla on havaittu vaikutuksia myös mielenterveyteen

Chen et al.: Ambient air pollution and daily hospital admissions for mental disorders in Shanghai, China, Science of the Total Environment 613–614, 324–330, 2018

Percent change in hospital admissions (%)

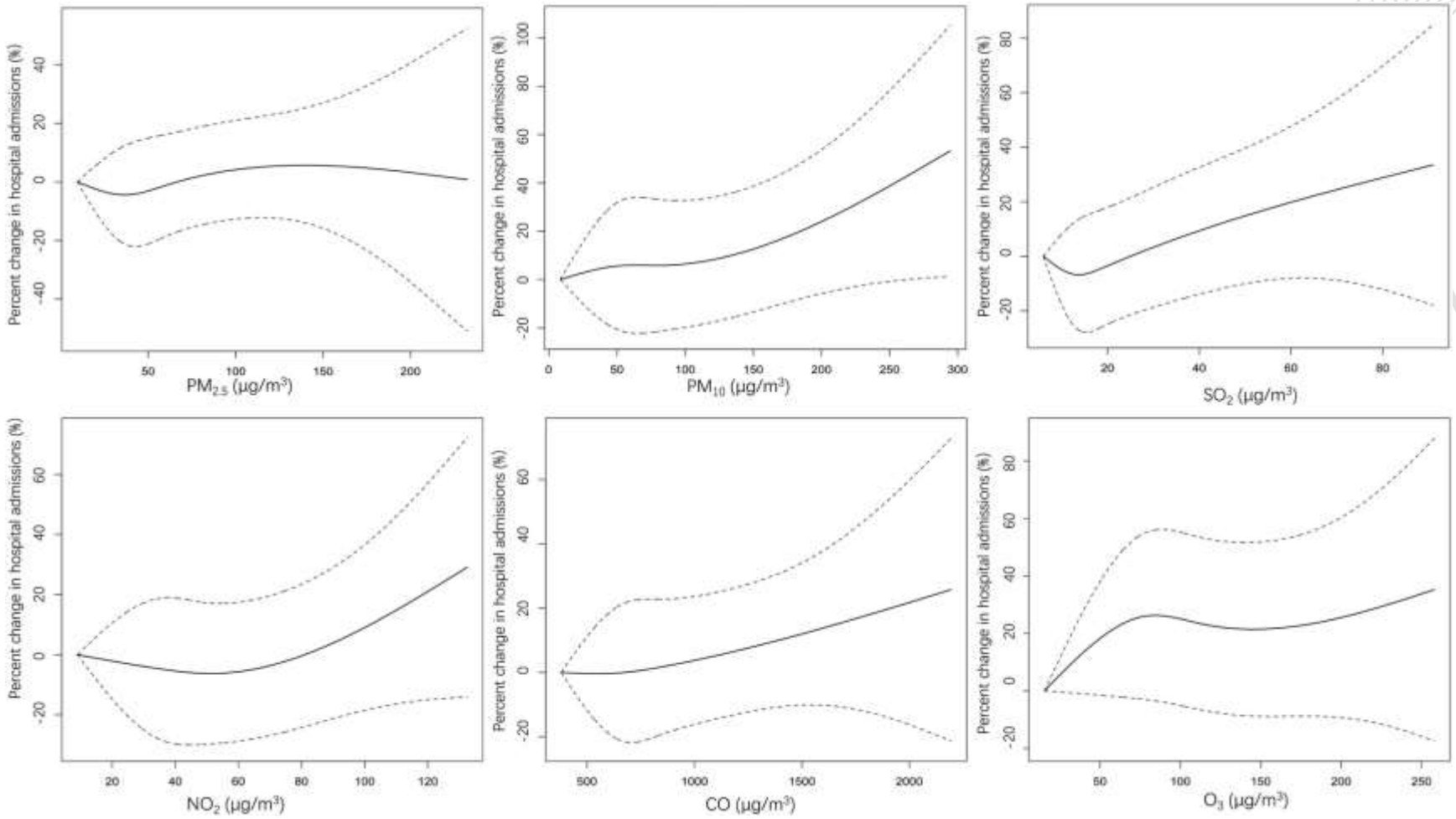

Fig. 1. The concentration–response relationship curves between air pollutants (lag 01 day) and daily hospitalizations for mental disorders.

Trendit näyttävät kääntyvän puhtaampaan. Esimerkkejä.

Environ. Res. Lett. **11** (2016) 114002

Recent reduction in NO_x emissions over China: synthesis of satellite observations and emission inventories

Fei Liu[1,2], Qiang Zhang[3], Ronald J van der A[2], Bo Zheng[1], Dan Tong[3], Liu Yan[3], Yixuan Zheng[3] and Kebin He[1]

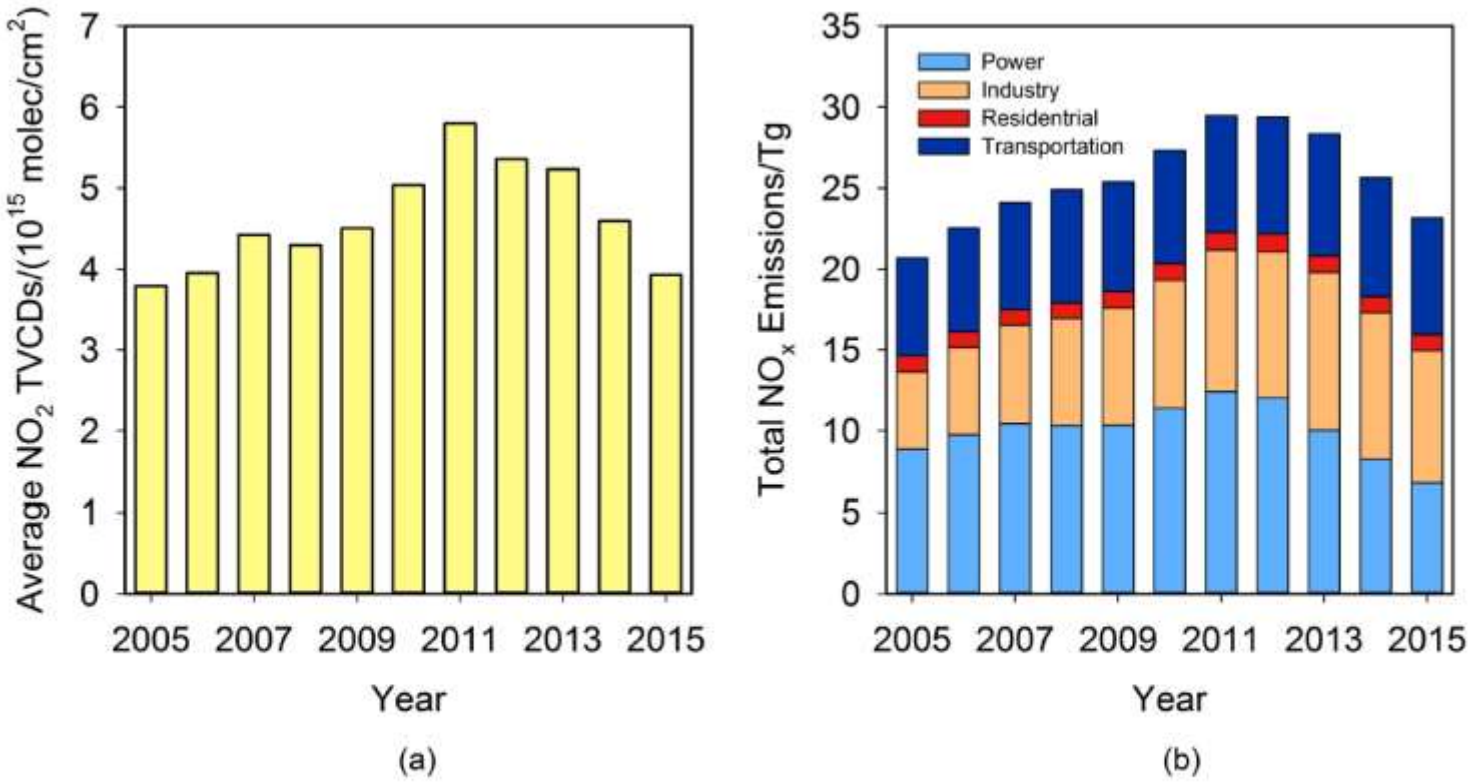

Figure 2. (a) Average OMI NO_2 column densities for China during 2005–2015. The background regions coloured in grey in figure 1 are removed from calculation. (b) Total anthropogenic NO_x emissions by sector for China during 2005–2015. The emission data are derived from the MEIC model.

Trendit näyttävät kääntyvän puhtaampaan. Esimerkkejä.

Zhang, J., J. S. Reid, R. Alfaro-Contreras, and P. Xian: Has China been exporting less particulate air pollution over the past decade?, Geophys. Res. Lett., 44, 2941–2948, 2017.

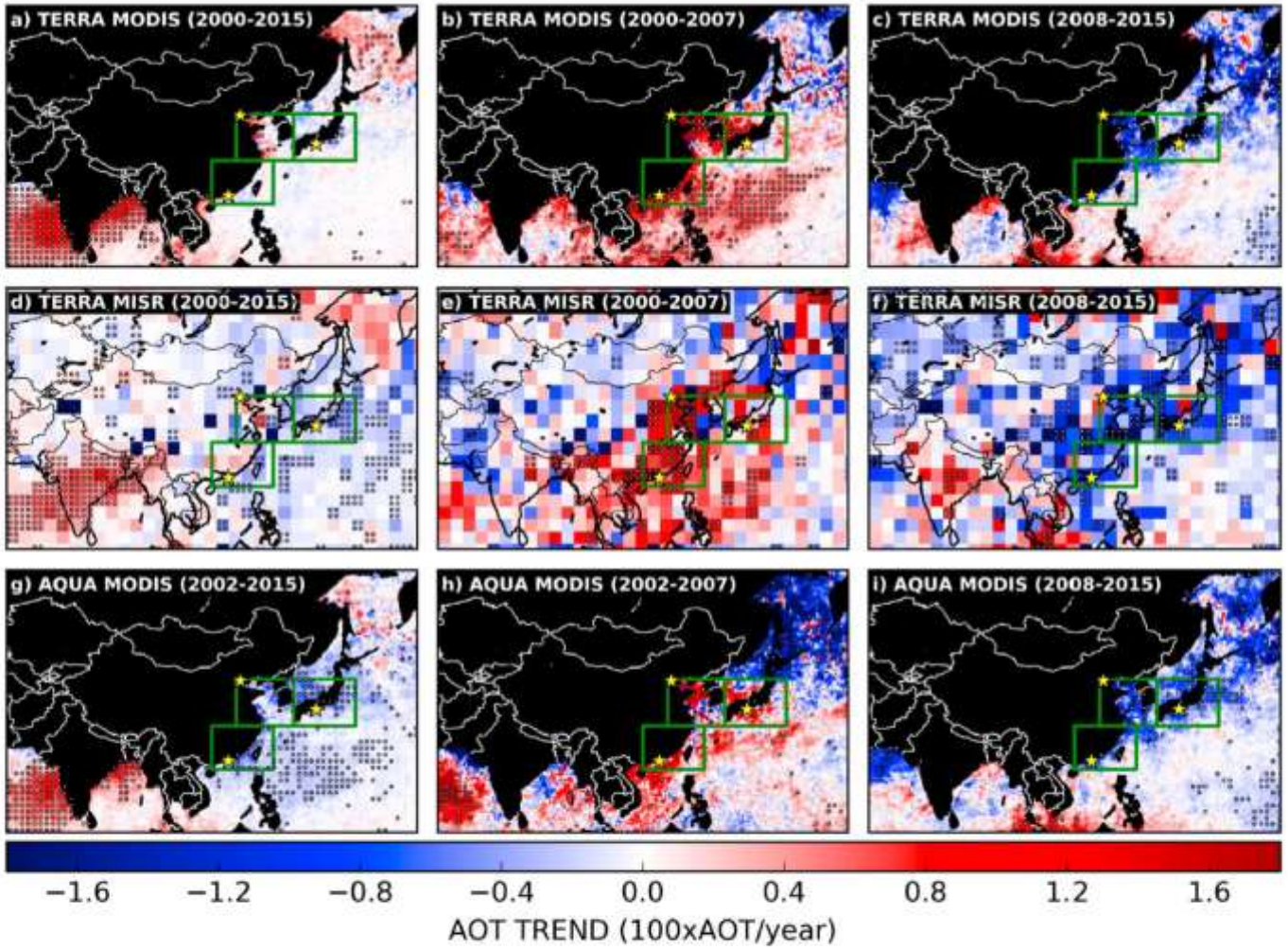

Figure 1. The spatial distributions of AOT trends at a spatial resolution of 0.5 × 0.5° (latitude/longitude) over Asia using (a) Terra MODIS DT data for 2000–2015, (b) Terra MODIS DT data for 2000–2007, (c) Terra MODIS DT data for 2008–2015, (d)–(f) similar to Figures 1a–1c but using MISR data (3 × 3°, latitude/longitude), (g) Aqua MODIS DT data for 2002–2015, (h) Aqua MODIS DT data for 2002–2007, and (i) Aqua MODIS DT data for 2008–2015. The green boxes show the three selected regions including the Northeast Coast of China, Southeast Coast of China, and Japan regions. The dotted regions are regions with statistically significant trends at a 95% confident interval. The Shirahama, XiangHe, and HongKong AERONET sites are also highlighted as yellow stars.

Satelliittidata-analyysi

Aerosolin optisen paksuuden poikkeama tarkastelujakson (2000 – 2015) keskiarvosta

Trendit näyttävät kääntyvän puhtaampaan. Esimerkkejä.

Zhang, J., J. S. Reid, R. Alfaro-Contreras, and P. Xian: Has China been exporting less particulate air pollution over the past decade?, Geophys. Res. Lett., 44, 2941–2948, 2017.

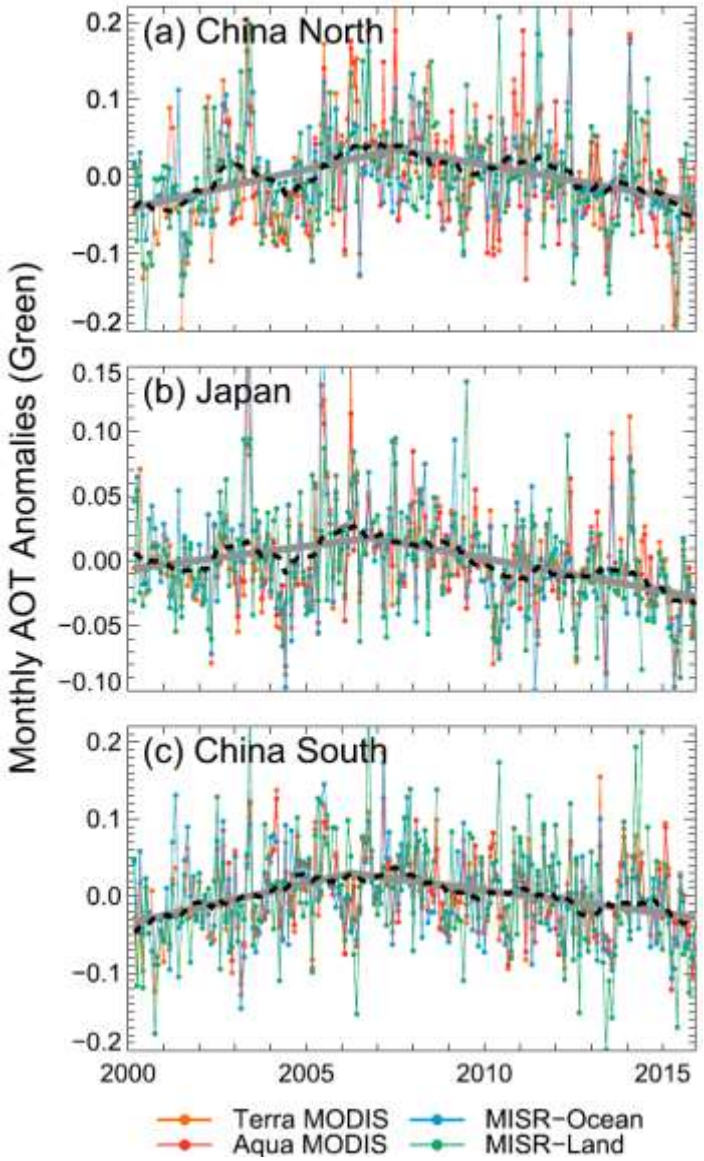

Satelliittidata-analyysi

Aerosolin optisen paksuuden poikkeama tarkastelujakson (2000 – 2015) keskiarvosta

Figure 2. Time series of deseasonalized Terra MODIS DT, Aqua MODIS DT, Terra MISR (over Land), and Terra MISR (over Ocean) AOTs for three selected regions: (a) Northeast Coast of China, (b) Japan, and (c) Southeast Coast of China. Ensemble means of the boxcar averages for AOT anomalies from Terra MODIS; over land and over ocean MISR are also shown in black dashed lines. The thick solid grey lines show the piecewised linear fits through those ensemble means. "Green" means the Green channel, or the 550 nm channel for MODIS and 558 nm channel for MISR.

Suuren mittakaavan kenttäkokeita

Mahdollisia Kiinassa ...

- Olympialaiset 2008
- APEC (Asia-Pacific Economic Cooperation (APEC) -kokous 2014)
- YOG 2014 (Youth Olympic Games 2014, Nanjing)
- ...

Sun et al.: **“APEC Blue”**: Secondary Aerosol Reductions from Emission Controls in Beijing, Sci. Rep., 6, 20668, doi:10.1038/srep20668, 2016

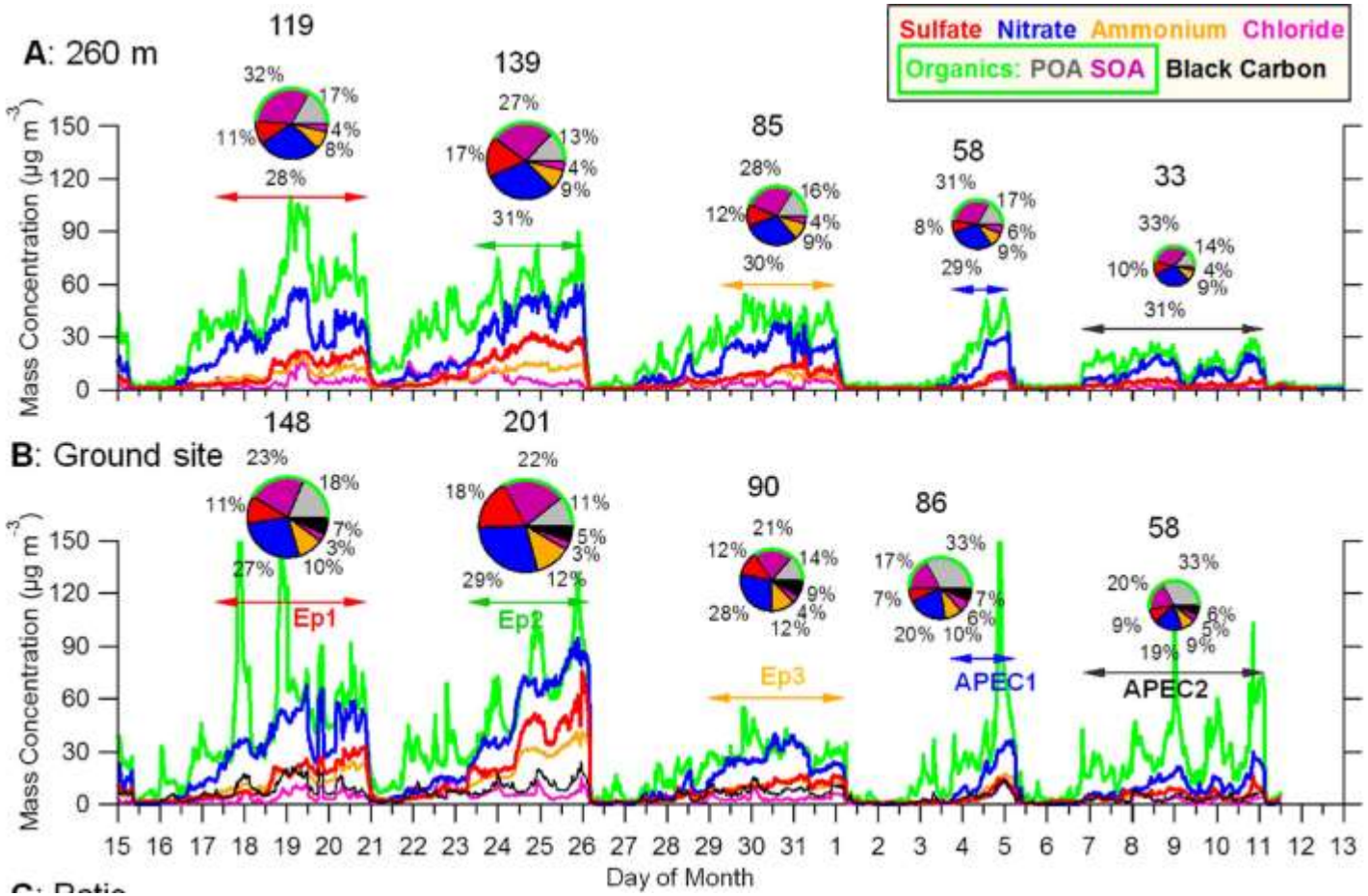

Figure 1. Aerosol particle composition before and during APEC. Time series of aerosol species, including SOA, POA, sulfate, nitrate, ammonium, chloride, and black carbon in PM_1 at (**A**) 260 m and (**B**) the ground site. The pie charts present the average chemical composition of PM_1 for five episodes as marked in the Figure, and the numbers on the top of pie chart are the average total PM_1 mass concentration in microgram per cubic meters. (**C**) shows the concentration ratio of each aerosol species between 260 m and the ground site during each episode. (**D**) shows the average difference in aerosol concentration for each episode compared to the average of all five episodes at 260 m and the ground site. The numbers show the percent change in each chemical species for the two episodes during the APEC.

15.10. - 13.11., 2014

Zhou, DR., Li, B., Huang, X., Virkkula, A., Wu, HS., Zhao, QY., Zhang, J., Liu, Q., Li, L., Li, CY., Chen, F., Yuan, SY., Qiao, YZ., Shen, GF., Ding, AJ.: The Impacts of Emission Control and Regional Transport on PM2.5 Ions and Carbon Components in Nanjing during the 2014 Nanjing Youth Olympic Games, AAQR, 17, 730 – 740, 2017.

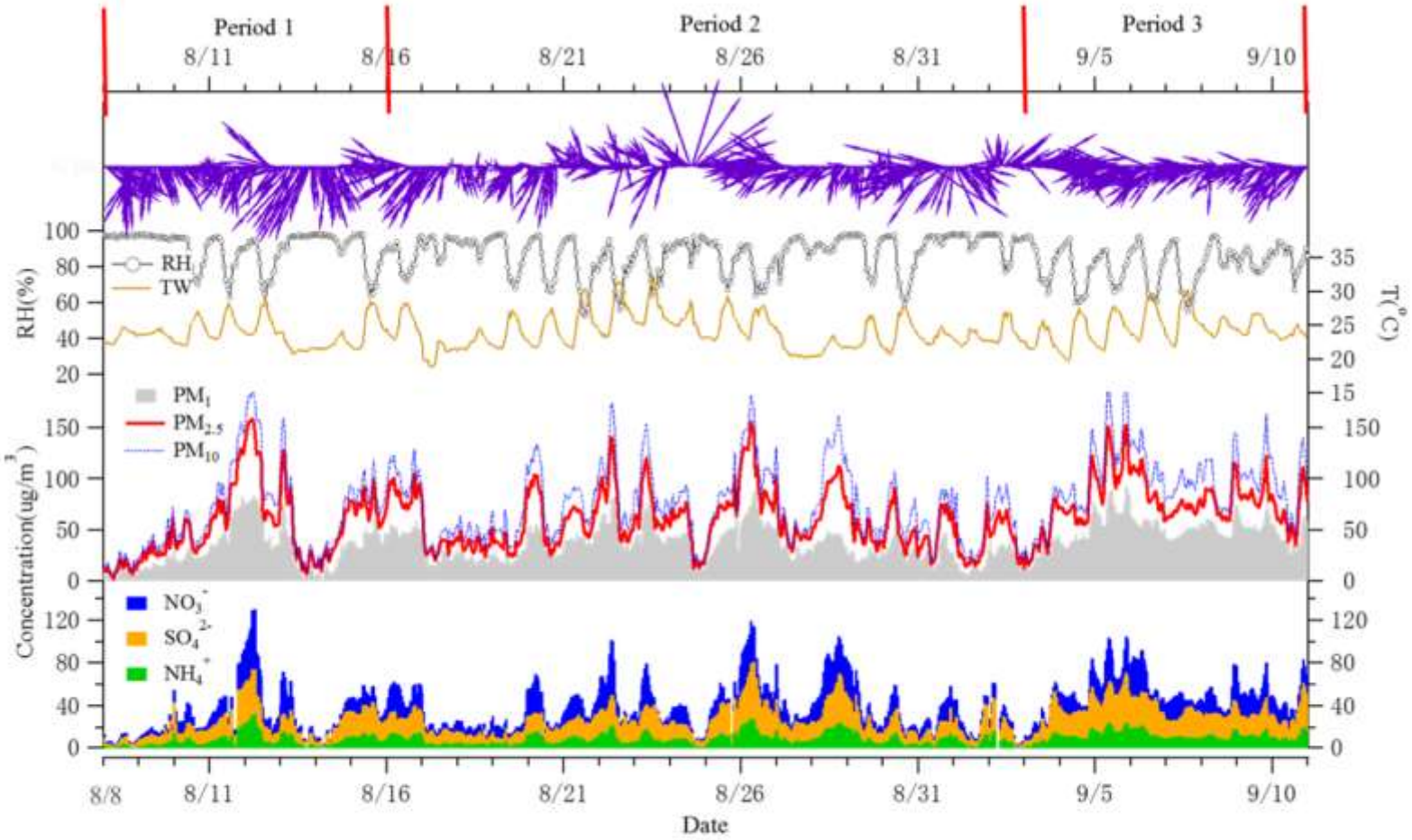

Fig. 2. Time series of NO_3^-, SO_4^{2-}, NH_4^+, PM_1, $PM_{2.5}$, PM_{10} with relative humidity (RH), air temperature (T), wind speed and direction at JAES during the study period. Note: Period 1- The pre-emission control period with limited reduction conducted. Period 2- The period of strict emission control. Period 3- The period without specific emission reduction.

Zhou, DR., Li, B., Huang, X., Virkkula, A., Wu, HS., Zhao, QY., Zhang, J., Liu, Q., Li, L., Li, CY., Chen, F., Yuan, SY., Qiao, YZ., Shen, GF., Ding, AJ.: The Impacts of Emission Control and Regional Transport on PM2.5 Ions and Carbon Components in Nanjing during the 2014 Nanjing Youth Olympic Games, AAQR, 17, 730 – 740, 2017.

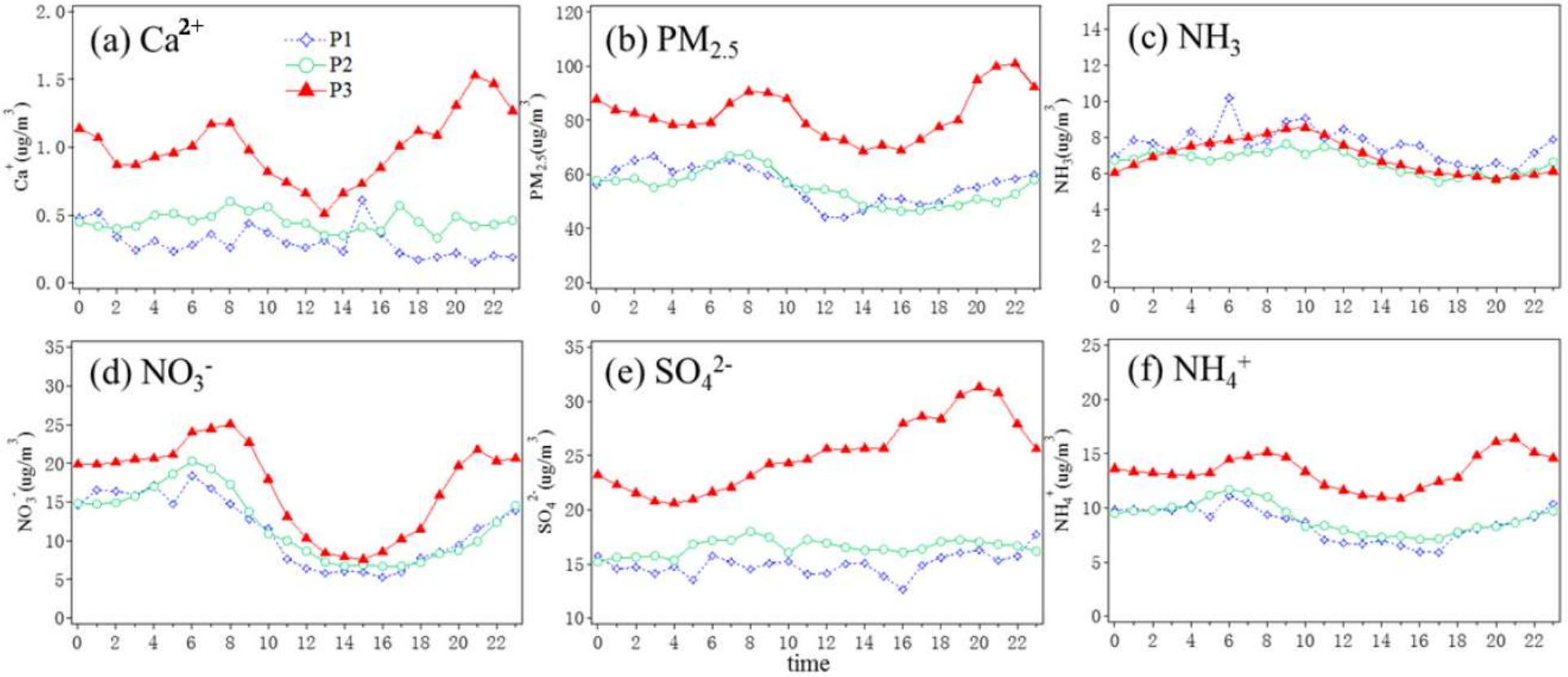

Fig. 3. Averaged diurnal variations of (a) Ca^{2+}, (b) $PM_{2.5}$, (c) NH_3, (d) NO_3^-, (e) SO_4^{2-} and (f) NH_4^+ in the three periods.

Zhou, DR., Li, B., Huang, X., Virkkula, A., Wu, HS., Zhao, QY., Zhang, J., Liu, Q., Li, L., Li, CY., Chen, F., Yuan, SY., Qiao, YZ., Shen, GF., Ding, AJ.: The Impacts of Emission Control and Regional Transport on PM2.5 Ions and Carbon Components in Nanjing during the 2014 Nanjing Youth Olympic Games, AAQR, 17, 730 – 740, 2017.

Table 1. Mean concentrations and standard deviations (Mean ± SD) of fine particle NO_3^-, SO_4^{2-}, NH_4^+ and Ca^{2+}, PM_1, $PM_{2.5}$, PM_{10}, SO_2, NO_2, ratio of NO_3^-/SO_4^{2-}, CE/AE with meteorological parameters during three periods in Nanjing.

Mean ± SD (μg m^{-3})	P1	P2	P3
PM_1	35.5 ± 20.7	33.4 ± 15.4	52.6 ± 13.1
$PM_{2.5}$	62.0 ± 34.5	55.1 ± 27.3	82.4 ± 22.5
PM_{10}	75.0 ± 41.3	70.2 ± 34.1	104.7 ± 28.8
NO_3^-	12.79 ± 10.87	12.12 ± 9.9	17.18 ± 9.01
SO_4^{2-}	16.34 ± 8.48	16.54 ± 9.17	25.12 ± 7.31
NH_4^+	9.34 ± 5.90	9.02 ± 5.36	13.44 ± 3.99
Ca^{2+}	0.20 ± 0.19	0.45 ± 0.32	1.00 ± 0.44
NO_3^-/SO_4^{2-}	0.75 ± 0.44	0.74 ± 0.42	0.72 ± 0.37
CE/AE	0.95 ± 0.09	0.98 ± 0.08	1.02 ± 0.03
NH_3	7.6 ± 2.7	6.6 ± 2.3	6.9 ± 2.0
NO_2	30.1 ± 12.0	31.6 ± 13.6	41.7 ± 17.0
SO_2	9.7 ± 6.1	9.8 ± 6.2	18.1 ± 6.9
T (°C)	24 ± 2.1	23.9 ± 2.6	24.7 ± 2.2
RH (%)	88.9 ± 9.9	87.1 ± 10.8	81.0 ± 10.6

AQI	Air Pollution Level
0 - 50	Good
51 -100	Moderate
101-150	Unhealthy for Sensitive Groups
151-200	Unhealthy
201-300	Very Unhealthy
300+	Hazardous

$$\frac{82.4-55.1}{55.1}100\% = 49.5\%$$

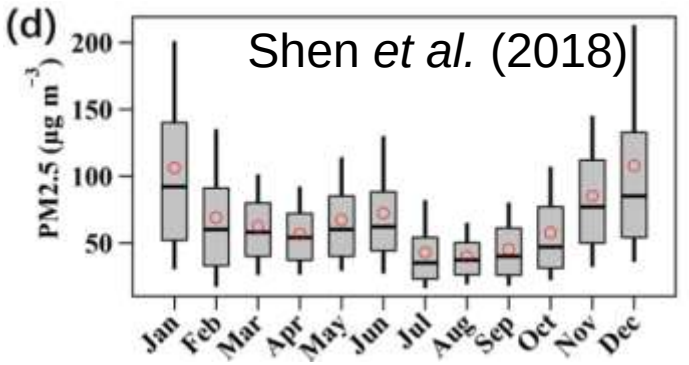

Petäjä, T., Järvi, L., Kerminen, V.-M., Ding, A. J., Sun, J. N., Nie, W., Kujansuu, J. , Virkkula, A., Yang, X., Fu, C.B., Zilitinkevich, S., and Kulmala, M. (2016). Enhanced air pollution via aerosol-boundary layer feedback in China. *Scientific Reports*, *6*, 18998. http://doi.org/10.1038/srep18998.

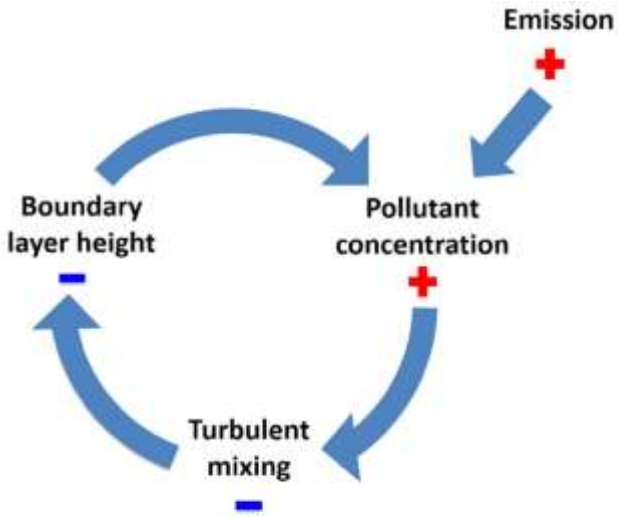

Figure 1. A schematic figure of the feedback mechanism initiated by the increased aerosol concentration in the boundary layer leading to lower boundary layer height and hence elevated aerosol concentrations.

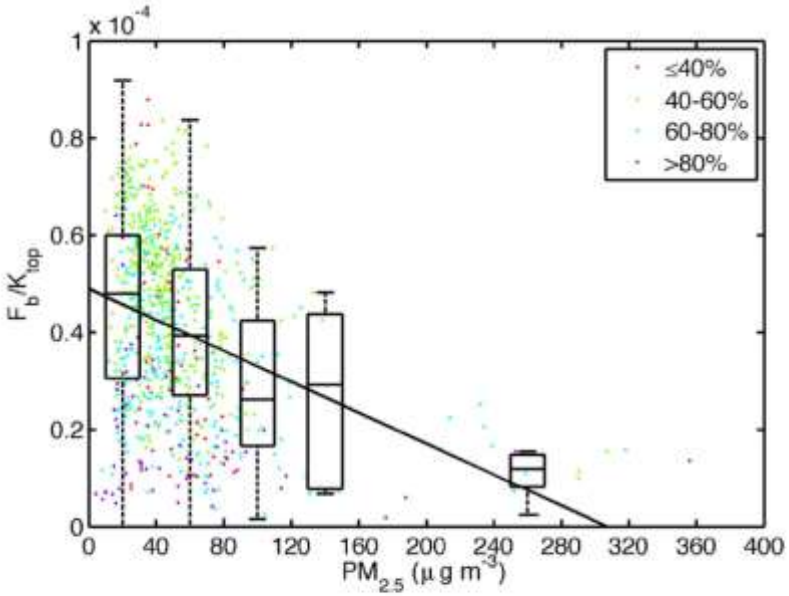

Figure 3. Observed dependency of the ratio between the turbulent vertical flux (F_b) and the solar radiation at the top of the atmosphere (K_{top}) as a function on observed particulate mass ($PM_{2.5}$) concentration. The

Ding, A. J., Huang, X., Nie, W., Sun, J. N., Kerminen, V. M., Petäjä, T., Su, H., Cheng, Y. F., Yang, X.-Q., Wang, M.H., Chi, X. G.,Wang, J. P., Virkkula, A., Guo, W. D., Yuan, J., Wang, S. Y., Zhang, R. J., Wu,Y.F., Song, Y., Zhu, T., Zilitinkevich, S., Kulmala, M., and Fu., C. B. (2016), Enhanced haze pollution by black carbon in megacities in China, Geophys. Res. Lett. , 43, doi:10.1002/2016GL067745

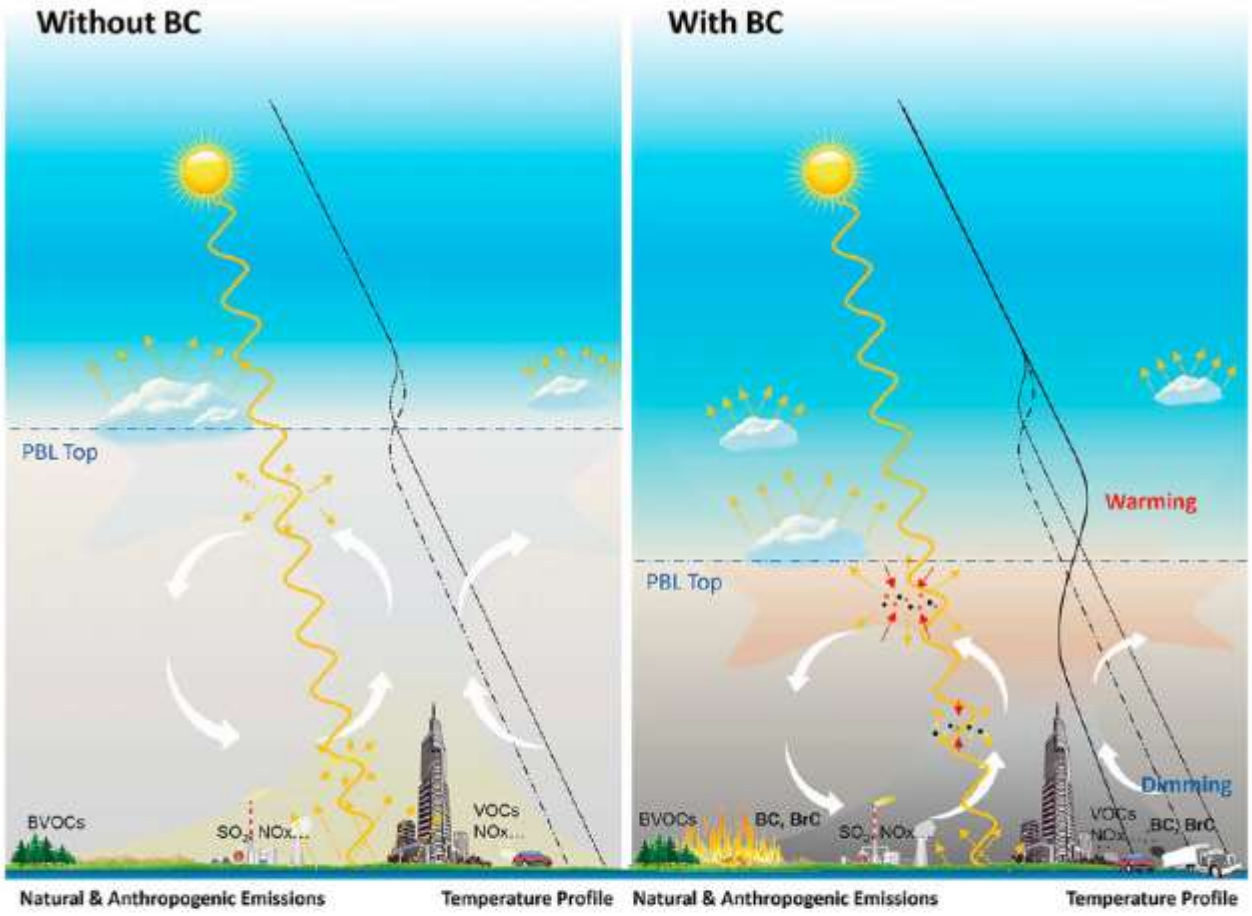

Figure 5. Aerosol-PBL feedback loop for the scenarios without and with BC emission in a megacity. Black lines show the vertical profile of air temperature (solid, dash-dotted and dotted lines for the scenarios with BC, with aerosols except for BC and without aerosols, respectively). Yellow dashed arrows show the reflection of solar ration by the ground surface, clouds, and scattering aerosols. Red arrows show the absorption of solar radiation by absorbing aerosols like BC and BrC. The blue dash-dotted line indicates the top of PBL. White arrows indicate the vertical ventilation of urban plumes induced by circulations or large eddies induced by the urban heat island effect. The difference in the color of urban plumes means different chemical compositions: the case on the right has more BC (or BrC) from sources like biomass burning, industry, and diesel vehicles, along with more aged air in the upper PBL.

Wang, J., Virkkula, A., Gao, Y., Lee, S., Shen, Y., Chi, X., Nie, W., Liu, Q., Xu, Z., Huang, X., Wang, T., Cui, L., and Ding, A.: Observations of aerosol optical properties at a coastal site in Hong Kong, South China, Atmos. Chem. Phys., 17, 2653-2671, doi: 10.5194/acp-17-2653-2017, 2017

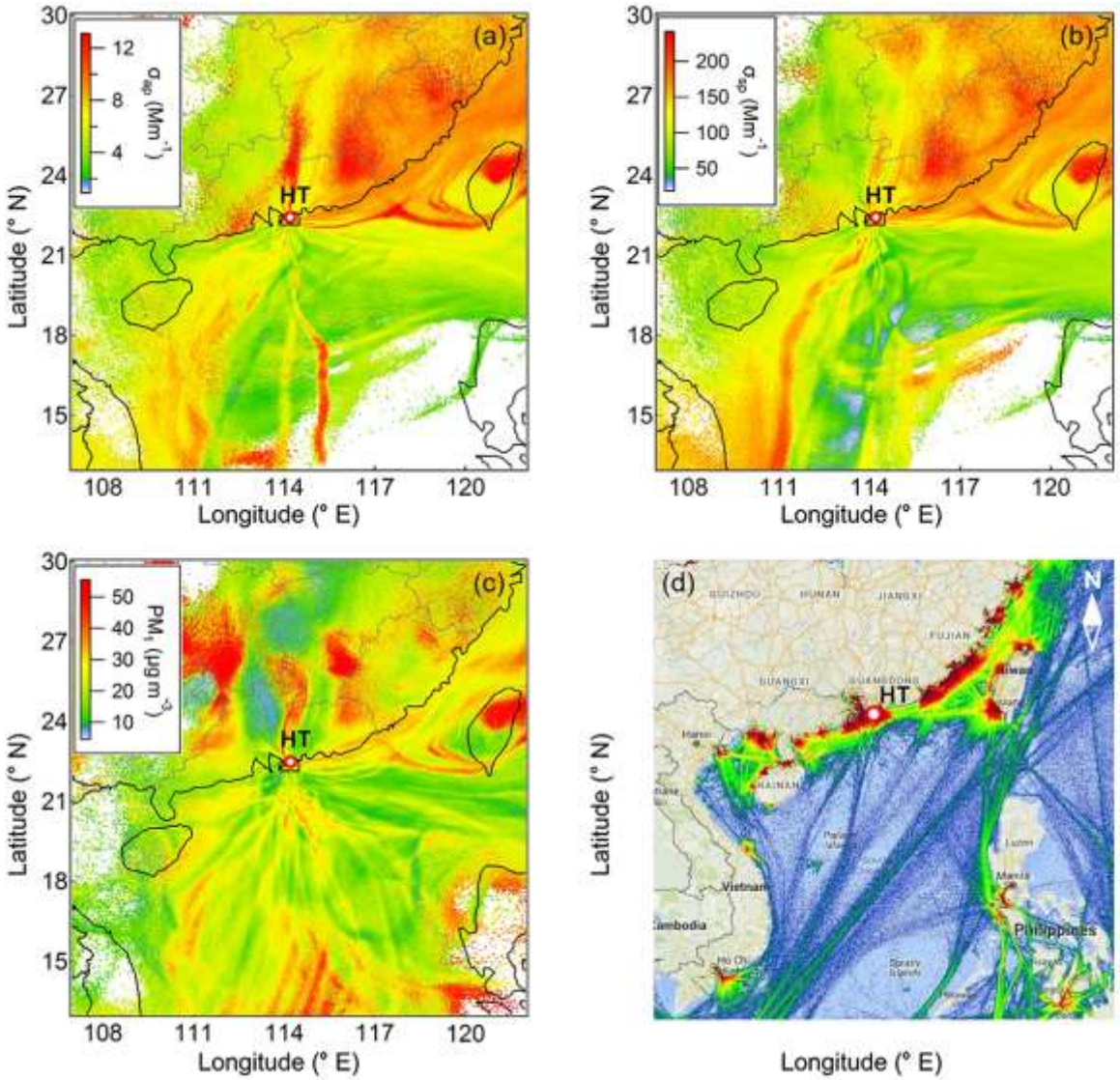

Figure 12. Map of average property$_{\text{retroplume}}$ for **(a)** σ_{ap}, **(b)** σ_{sp}, and **(c)** PM_1 (the non-colored areas were where the total retroplume was smaller than 10^{-12} mass m^{-3} h^{-1} (i.e., air plumes barely passed through these regions). Due to the different time period of valid data from UFP, the non-colored areas were slightly different in **(c)**. **(d)** Density map showing the ship routes near Hong Kong during 2013 and 2014.

Shen, Y., Virkkula, A., Ding, A., Wang, J., Chi, X., Nie, W., Qi, X., Huang, X., Liu, Q., Zheng, L., Xu, Z., Petäjä, T., Aalto, P. P., Fu, C., and Kulmala, M.: Aerosol optical properties at SORPES in Nanjing, east China, Atmos. Chem. Phys., 18, 5265-5292, 2018.

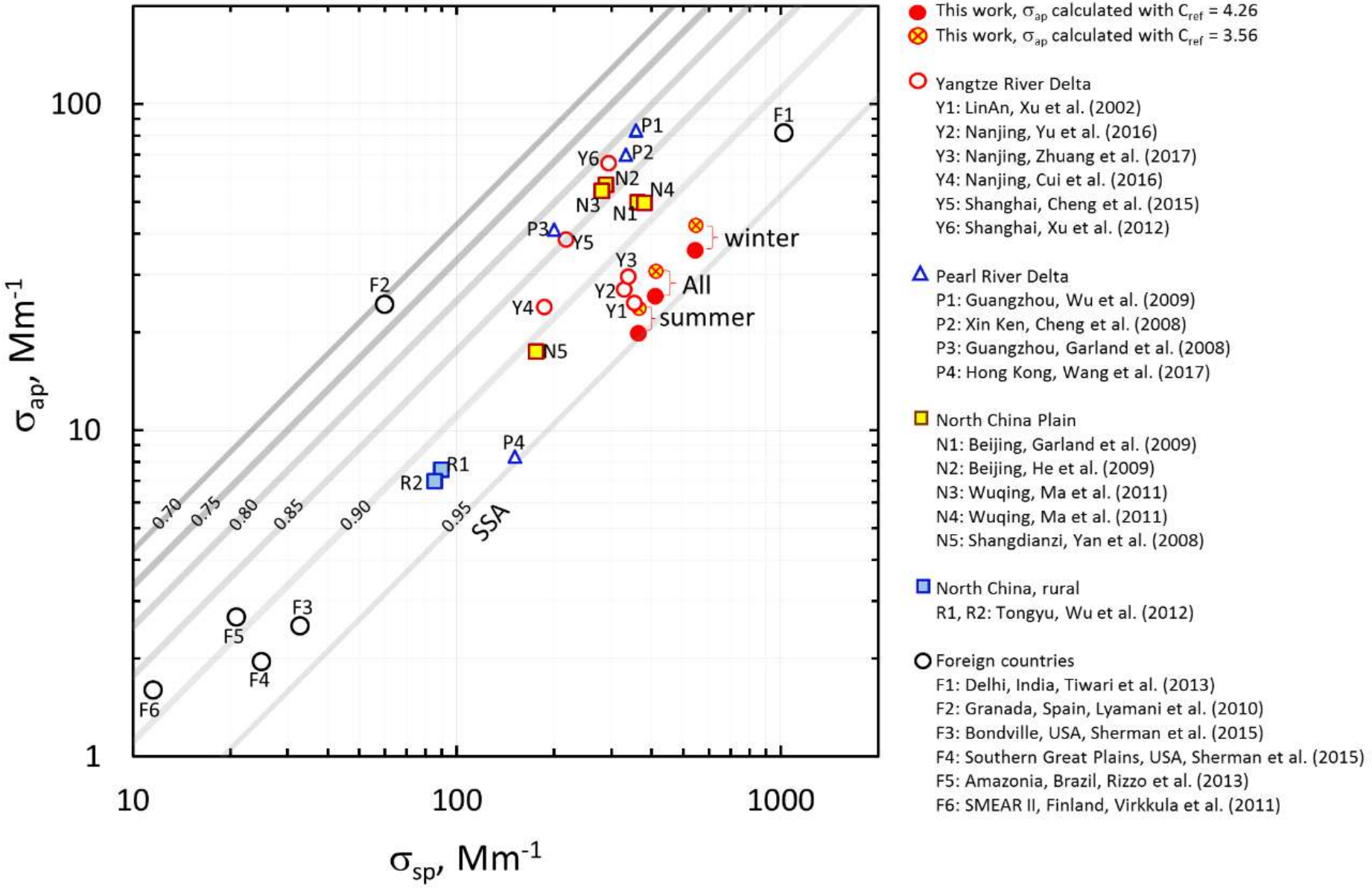

Shen, Y., Virkkula, A., Ding, A., Wang, J., Chi, X., Nie, W., Qi, X., Huang, X., Liu, Q., Zheng, L., Xu, Z., Petäjä, T., Aalto, P. P., Fu, C., and Kulmala, M.: Aerosol optical properties at SORPES in Nanjing, east China, Atmos. Chem. Phys., 18, 5265-5292, 2018.

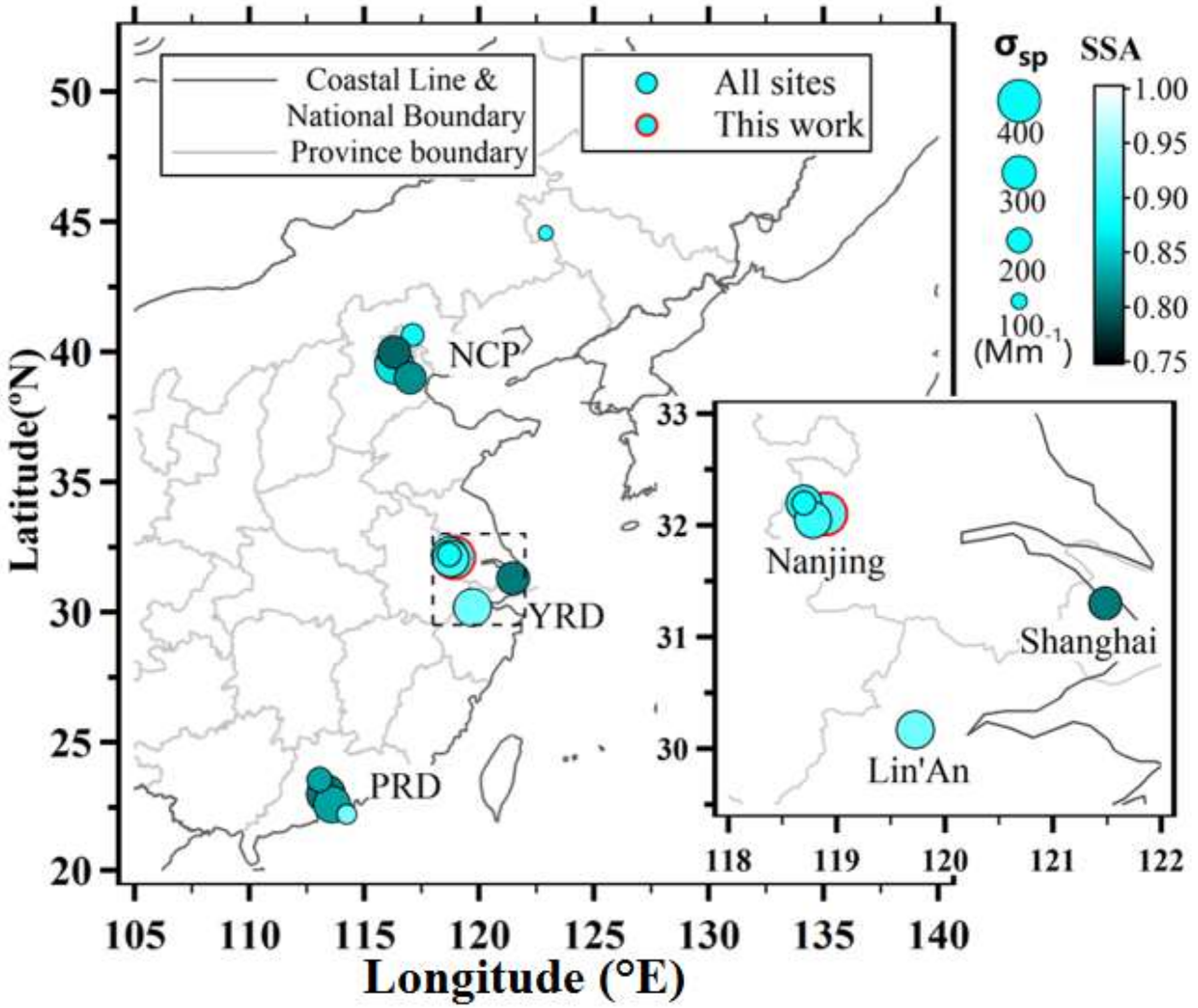

SORPES - Station for Observing Regional Processes of the Earth System

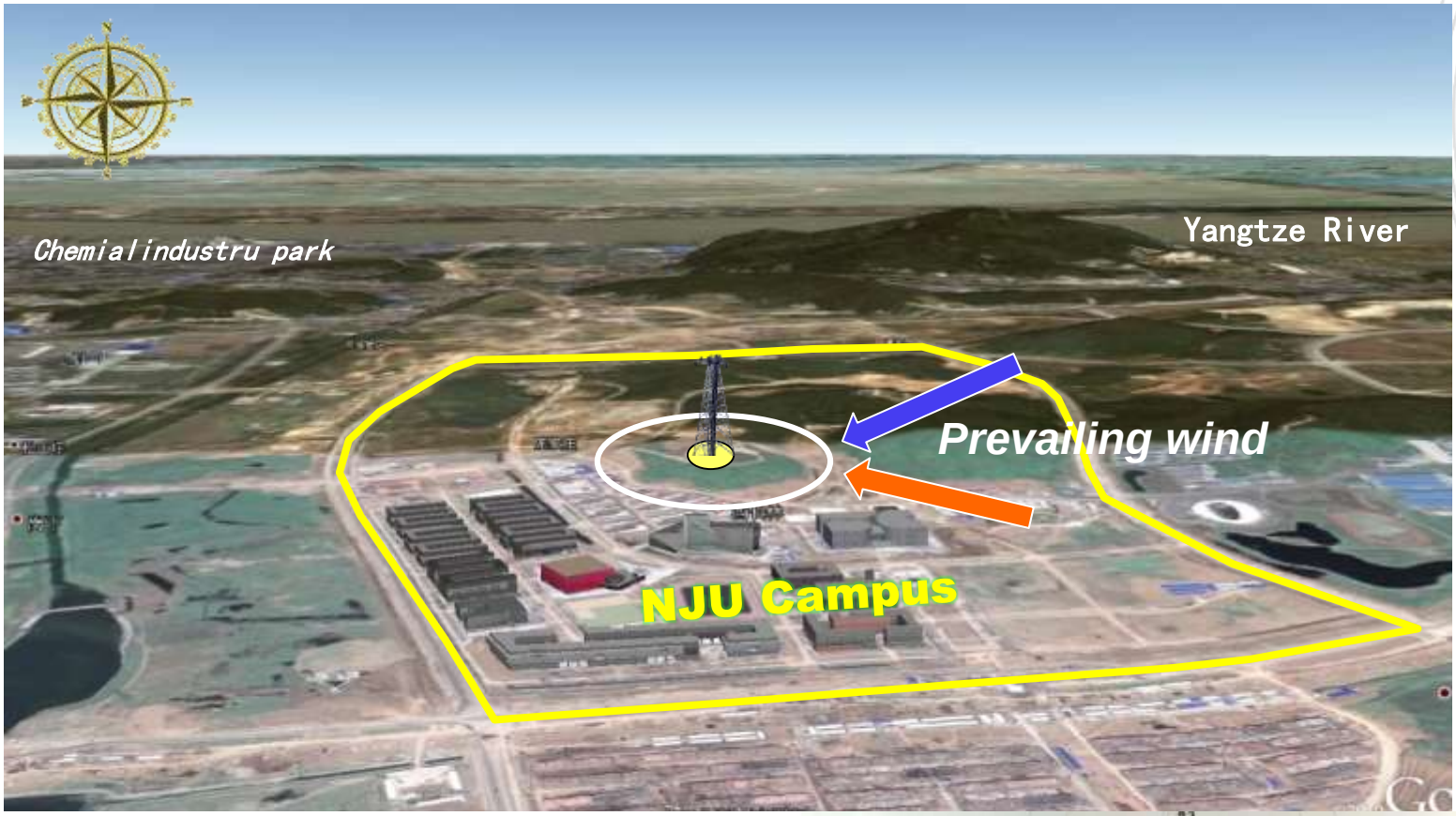

Atmospheric components

N E S W

Meteorological parameters

Tower 75m

Weather Radar

Instruments at SORPES

Aerosol:

- ✓ SHARP (PM2.5 mass)
- ✓ PSM (1-1000 nm);
- ✓ AIS (0.8-42 nm);
- ✓ DMPS (6-800 nm);
- ✓ APS (500-20000 nm);
- ✓ Nephlometer, Aethalometer;
- ✓ MPL radar;
- ✓ MARGA (on line PM2.5 ions);
- ✓ Sunset EC/OC (on line);
- ✓ Filter samplers (PM_1, $PM_{2.5}$, size resolved)

❖ Others

- ✓ Precipitation chemistry
- ✓ Deposition of pollens

❖ Gases

- ✓ O_3, CO, CO_2, SO_2, NO-NO_x-No_y
- ✓ Mini-DOAS
- ✓ NH_3, HONO etc. using MARGA
- ✓ H_2O isotope

Meteorology

- ✓ Automatic weather stations
- ✓ Multi-layer met. (WD, WS, RH, T)
- ✓ Flux (CO_2, H_2O, soli heat)
- ✓ Global radiation/Reflected radiation/Scattered radiation/Direct radiation/UVB
- ✓ Soil temperature/soil water content
- ✓ Sounding (Wind, RH, T in intensive campaign)
- ✓ Weather radar
- ✓ Doppler wind profile radar